Cryptogamie, Algologie, 2017, 38 (4): 285-323

Cryptic cyanobacterial diversity in the giant cave (Trieste, Italy): the new genus *Timaviella* (Leptolyngbyaceae)

*Katia SCIUTO *, Emanuela MOSCHIN & Isabella MORO*

Department of Biology, University of Padova, via U. Bassi 58/B, 35131 Padova (Italy)

Abstract – The microflora of hypogean environments has been studied increasingly worldwide. However, some sites have hardly been examined or not studied at all; this is the case for the Giant Cave, a Karst show cave located near Trieste, Italy. In the present study we began characterizing the Giant Cave *Lampenflora* by using a polyphasic approach, focusing, in particular, on three *Leptolyngbya*-like strains named GR2, GR4, and GR13. Light and electron microscopic observations were carried out and the water-soluble pigment composition was analysed. Phylogenetic reconstruction, based on the 16S rRNA gene and the 16S-23S ITS region, was performed to better understand the taxonomic position of these strains, complemented by 16S-23S ITS secondary structure analysis. Ecological and geographical data for the investigated strains and for the other cyanobacterial strains grouping with them in the phylogenetic reconstructions were also considered. Based on the results, strain GR2 was ascribed to the species *Heteroleibleinia purpurascens* (Hansgirg) Anagnostidis & Komárek; strains GR4 and GR13 were attributed to a new genus of the family Leptolyngbyaceae, *Timaviella* Sciuto & Moro, gen. nov., and represented two distinct species: *Timaviella circinata* Sciuto & Moro and *Timaviella karstica* Sciuto & Moro.

16S rRNA / 16S-23S ITS / *Heteroleibleinia purpurascens* / hypogean environment / *Lampenflora* / *Timaviella*

INTRODUCTION

Caves are hypogean environments that can be considered extreme since the conditions are life-limiting, the most important factors being low nutrient input and scarcity/absence of light. A high relative humidity and a broadly constant temperature throughout the year are typical of caves (Mulec *et al.*, 2008; Lee *et al.*, 2012; Saiz-Jimenez, 2012). In caves the microflora colonizes different ecological niches, including water bodies and aerophytic habitats; the latter are represented by sediments, rocky surfaces, and artificial material. Substrate types play an important role in the selection of taxa (Mulec *et al.*, 2008).

The delicate equilibrium among the different biotic components (plants, animals, and microbes) of a cave is altered in show caves by visitors, who can bring organic input, and by the installation of associated infrastructure, like lamps (Mulec *et al.*, 2008; Saiz-Jimenez, 2012; Lamprinou *et al.*, 2014). In particular, artificial lighting favours the growth of microflora, the so-called *Lampenflora* (Dobát, 1963), even in the cave depths, where it otherwise would not develop.

* Corresponding author: katia.sciuto@unipd.it

doi/10.7872/crya/v38.iss4.2017.285

While at the cave threshold several types of organisms (e.g., microalgae, bryophytes, ferns) compete for sunlight, in the deepest recesses cyanobacteria are usually the only phototrophs. In show caves, these prokaryotes constitute most of the *Lampenflora* on calcareous surfaces, representing both the base of food chains and a possible threat to the cultural heritage (Smrž *et al.*, 2013; Lamprinou *et al.*, 2014).

Studies on microorganisms isolated from caves have highlighted that the particular conditions of these environments often lead to the selection of unusual taxa (Mulec *et al.*, 2008; Lee *et al.*, 2012); several new cyanobacterial genera and species were reported from caves and, more generally, from low light environments (e.g., Sant'Anna *et al.*, 1991; Hernández-Mariné & Canals, 1994; Asencio *et al.*, 1996; Lamprinou *et al.*, 2011, 2012a, 2012b, 2013; Zammit *et al.*, 2012; Saw *et al.* 2013; Hauer *et al.*, 2015; Miscoe *et al.*, 2016).

Recently, many caves have been thoroughly investigated worldwide (Lee *et al.*, 2012; Saiz-Jimenez, 2012; Hauer *et al.*, 2015), whereas some others have hardly been studied or are completely unknown; this is the case for the Giant Cave (Sgonico, Trieste, Italy). Over time, the artificial lighting has favoured the proliferation of microflora near the lamps, mostly represented by cyanobacteria. Part of the microflora could have already been present in the cave due to geological changes over time, while some could have been introduced by the traffic of people in the Giant Cave. Human transportation of microorganisms is often an underestimated factor, but people can bring new taxa into the cave, move taxa through the cave, and export taxa from the cave, thus altering the composition of the *Lampenflora*. In February 2012, a survey was started to study the *Lampenflora* of the Giant Cave with the collection of numerous samples and the isolation of different cyanobacterial and microalgal strains.

In this paper we report the characterization of three *Leptolyngbya*-like cyanobacteria isolated from this environment and temporarily named GR2, GR4, and GR13. The genus *Leptolyngbya* Anagnostidis & Komárek is a character-poor taxon that, based on molecular data, has undergone several revisions with the detection and separation of new genera (e.g., Perkerson *et al.*, 2011; Zammit *et al.*, 2012; Vaz *et al.*, 2015; Sciuto & Moro, 2016). The three isolated strains were investigated using a polyphasic approach, including morphological, ecological, biochemical, and molecular data. The molecular analyses were based on the 16S rRNA gene and the 16S-23S ITS region; moreover, the study of 16S-23S ITS secondary structures was also carried out. Strain GR2 was attributed to the species *Heteroleibleinia purpurascens* (Hansgirg) Anagnostidis & Komárek and the genus *Timaviella* Sciuto & Moro was erected for strains GR4 and GR13, which represent two distinct species: *Timaviella circinata* Sciuto & Moro and *Timaviella karstica* Sciuto & Moro.

MATERIALS AND METHODS

Study site

The Giant Cave ("Grotta Gigante" in Italian) is a Karst show cave located in the alpine area (Oriental Alps), in the municipality of Sgonico, Trieste, North-Eastern Italy; the main entrance coordinates are 45°42'35.62''N; 13°45'52.33''E.

The cave has an estimated age of around 10 million years. In 1995, it entered the *Guinness Book of Records* as the world's largest tourist cave, because of its central hall that reaches 98.5 m in height, 76.3 m in width, and is 167.6 m long. Several large stalactites and stalagmites are present in the cave and many of them have been named (e.g., the highest stalagmite, 12 m high, is "Colonna Ruggero" and a 7 m high stalagmite, famous for its form resembling a palm tree, is "Palma"). Stalagmites have a typical "pile of dishes" appearance due to water dropping from up to 80 m above and depositing calcium carbonate over a wide area. The temperature, constant throughout the year, is about 11°C and the relative humidity is 96% (http://www.grottagigante.it/).

Sampling, strain isolation, and culture setup

In February 2012, different samples of the microflora growing near the artificial lighting were collected by scratching the lithic surface with a stainless steel spatula and placed in Falcon tubes (50 mL). The light intensity at the exact position of each sampling, measured with a HD 9221 photoradiometer (Delta OHM S.r.l., Padova, Italy), ranged from 2 to 5 µmol photons m^{-2} s^{-1}. Strain isolation was accomplished by streaking each natural sample across an agar plate containing BG11 medium (Rippka *et al.*, 1979); after streaking, the agar plates were incubated and kept in a growth chamber at a constant temperature of 16°C, under a continuous light of 2-5 µmol photons m^{-2} s^{-1}, until colonies of cells appeared. Developed colonies were removed from the agar plate by a platinum loop under an inverted microscope (Leitz Diavert, Wetzlar, Germany). Cells were re-streaked on a new agar plate or, if the single colonies were unialgal/unicyanobacterial, they were rinsed in liquid BG11 medium to free the cells. Finally, liquid cultures of each isolated strain were set up with BG11 medium under the above reported culture conditions.

Among the isolated organisms, three cyanobacterial strains, named GR2, GR4, and GR13 (where the acronym "GR" stands for the Italian word "GRotta", cave), were the subject of this investigation. The three strains were deposited in the BCCM/ULC Cyanobacteria collection (Centre for Protein Engineering, University of Liège, Belgium), where they can be found under the following accession numbers: ULC400, ULC401, ULC402. Resin-embedded samples of strains GR2, GR4, and GR13 were obtained following Moro *et al.* (2010) and deposited at the Herbarium Patavinum (PAD), the herbarium of the Botanical Garden – University of Padova, under the following deposition numbers: A000628, A000629, A000630.

Amplification and sequencing of the 16S rRNA gene and 16S-23S ITS region

Culture aliquots of the three strains were ground in a mortar with liquid nitrogen and genomic DNA was extracted using the Genomic DNA Purification Kit (Thermo Fisher Scientific, Waltham, MA, USA) according to the manufacturer's instructions.

The 16S rRNA gene was amplified using the primer pair 16S1-16S2 (Ceschi-Berrini *et al.*, 2004), while the 16S-23S ITS region was amplified with the primer pair 322F-340R (Iteman *et al.*, 2000); the expected sizes for the amplicons were about 1450 bp for the 16S rRNA gene and from 650 to 950 bp for the 16S-23S ITS region. The PCR protocols were performed in 50 µl aliquots with the Taq DNA polymerase (Thermo Fisher Scientific, Waltham, MA, USA) according to the manufacturer's recommendations. Approximately 80 ng of template DNA was used

per reaction. The thermocycling conditions were the same as reported in Moro *et al.* (2007), for the 16S rRNA gene, and in Sciuto & Moro (2016), for the 16S-23S ITS region.

After observing the expected band on the electrophoretic gel, the corresponding amplification product was purified with the QIAquick PCR Purification kit (Qiagen, Hilden, Düsseldorf, Germany) prior to sequencing. DNA sequencing was performed at the BMR Genomics Sequencing Service (University of Padova) with the same primer pairs used in the amplification reactions. For the 16S rRNA gene, four additional internal primers were used as reported in Ceschi-Berrini *et al.* (2004).

The final consensus sequences were assembled using the SeqMan II program from the Lasergene software package (DNAStar©, Madison, WI, USA) and then compared with the sequences available at the INSD (International Nucleotide Sequence Database) using the BLAST tool (Altschul *et al.*, 1990).

The final 16S rRNA consensus sequences were 1343 bp for strain GR2, 1403 bp for strain GR4, and 1416 bp for strain GR13; the final 16S-23S ITS consensus sequences were 863 bp for strain GR2, 694 bp for strain GR4, and 675 bp for strain GR13. The obtained sequences were deposited in the INSD, through the ENA (European Nucleotide Archive) platform, with the following accession numbers: LT634148, LT634149, LT634150, for the 16S rRNA gene, and LT634151, LT634152, LT634153, for the 16S-23S ITS.

Phylogenetic analyses

Separate datasets were created for the 16S rRNA gene and 16S-23S ITS region, using the sequences of strains GR2, GR4, GR13, sequences found through the BLAST search, and other published sequences of strains belonging to genera of the family Leptolyngbyaceae. A sequence of the genus *Tapinothrix* (HQ132936), assigned to the family Heteroleibleiniaceae by Komárek *et al.* (2014), was also added to the 16S rRNA dataset. The 16S rRNA dataset included 100 sequences and the final alignment contained 713 aligned positions; sequences of strains belonging to the genus *Gloeobacter* were used as outgroup. For the 16S-23S ITS, 33 sequences were included in the dataset for a final alignment of 787 positions; due to the higher variability of this locus, representative sequences of the genera *Haloleptolyngbya* and *Nodosilinea*, which were at the base of the family Leptolyngbyaceae in the 16S rRNA tree, were used to root the phylogenetic reconstruction.

The obtained 16S-23S ITS sequences and the sequences retrieved from the INSD were checked for the presence of tRNAs with tRNAscan-SE (Lowe & Eddy, 1997; Schattner *et al.*, 2005) and the conserved domains/variable regions (D1, D1', D2, D3, D4, V2, boxB, boxA, D4, and V3) of this locus were detected following Iteman *et al.* (2000). A genomic region from the beginning of the D1 domain to the end of the D4 domain was considered in the ITS region phylogenetic analyses.

The 16S rRNA and 16S-23S ITS multiple alignments were generated with MUSCLE (Edgar, 2004) and are given as Supplementary Data (Figs S3 and S4, see doi/10.7872/crya/v38.iss4.2017.Suppl.Mat.).

Phylogenetic analyses based on Neighbor Joining (NJ) and Maximum Parsimony (MP) methods were performed with MEGA version 5 (Tamura *et al.*, 2011). The 16S rRNA dataset had 185 parsimony-informative sites in 713 aligned positions, and the 16S-23S ITS dataset had 343 parsimony-informative sites in 787 aligned positions. Maximum Likelihood (ML) analyses were performed with

PHYML version 3.065 (Guindon & Gascuel, 2003) and Bayesian Inference (BI) analyses were carried out using MrBayes version 3.1.2 (Ronquist & Huelsenbeck, 2003).

For ML and BI analyses, the models that best fit our data were found using jModelTest version 0.1.1 (Posada & Crandall, 1998; Posada & Buckley, 2004; Posada, 2008) under the BIC criterion (Schwarz, 1978). For the 16S rRNA dataset, the model that best fit the data was TrN + I + G and the following parameters were implemented: nucleotide frequencies as freqA = 0.2624, freqC = 0.1875, freqG = 0.3137, freqT = 0.2363; substitution rate matrix with A-C substitutions = 1.0000, A-G = 2.3871, A-T = 1.0000, C-G= 1.0000, C-T = 3.6598, G-T = 1.0000; proportion of sites assumed to be invariable = 0.5350; gamma shape = 0.5230. For the 16S-23S ITS dataset, the model that best fit the data was TPM2uf + G and the following parameters were implemented: nucleotide frequencies as freqA = 0.3148, freqC = 0.1609, freqG = 0.2394, freqT = 0.2849; substitution rate matrix with A-C substitutions = 2.1211, A-G = 4.4077, A-T = 2.1211, C-G= 1.0000, C-T = 4.4077, G-T = 1.0000; proportion of sites assumed to be invariable = 0; gamma shape = 0.3440.

The nexus files for the BI analyses were generated with Mesquite version 2.71 (Maddison & Maddison, 2009). The analyses included two separate concurrent MCMC runs, each composed of four chains (three heated and one cold). Each Markov chain ran for 10×10^6 generations for the 16S rRNA dataset and 5×10^6 generations for the 16S-23S ITS dataset, with trees sampled every 100 generations. At the end of each run, we considered the sampling of the posterior distribution to be adequate if the average standard deviation of the split frequencies was ≤ 0.01. The first 25000 trees for the 16S rRNA locus and 12500 trees for the 16S-23S ITS were discarded as burn-in, as determined by the stationarity of the lnL assessed using Tracer version 1.5 (Rambaut & Drummond, 2007). Consensus topologies and posterior probabilities (PP) values were calculated from the remaining trees. Nonparametric bootstrap (BT) re-sampling (Felsenstein, 1985) was used to test the robustness of the NJ, MP, and ML tree topologies (1000 BT replicates). Final images of the phylogenetic reconstructions were prepared for publication with CorelDRAW X4.

Secondary structure prediction

The hypothetical secondary structures of the 16S-23S ITS region were estimated as reported in Sciuto & Moro (2016), using the program RNAstructure version 5.6 (Reuter & Mathews, 2010) with default conditions (absolute temperature for structure prediction = 37°C; maximum loop size = 30 unpaired nucleotides; maximum % energy difference = 10; maximum number of structures = 20; window size = 0). In some cases, the predictions obtained with RNAstructure were constrained in some parts to make the structures more congruent and comparable among them. The obtained secondary structures were visualized with VARNA version 3.9 (Darty *et al.*, 2009) and depicted with CorelDRAW X4.

Microscopy

Culture aliquots of the three strains were observed with a light microscope (LM) Leica 5000 (Wetzlar, Germany), equipped with a digital image acquisition system. Further aliquots of the three strains were fixed in 3% glutaraldehyde in

0.1 M cacodylate buffer (pH 6.9) and prepared for electron microscopy analyses as reported in Moro *et al.* (2010). Scanning electron microscope (SEM) observations were carried out with a JSM-6490 JEOL (Akishima, Tokyo, Japan) microscope, operating at 25 kV, and transmission electron microscope (TEM) observations were performed with a FEI Tecnai G2 (Hillsboro, Oregon, USA) microscope, operating at 100 kV. Micrographs of the three strains were prepared for publication with CorelDRAW X4. Morphological classification of the strains was based on Komárek & Anagnostidis (2005) and Komárek *et al.* (2014).

Capability of strain GR2 to attach to the substrate

To evaluate whether strain GR2 was able to attach to the substrate by one end of the filaments, an experiment was carried out as follows. Small fragments of calcareous rock were washed with a sodium hypochlorite solution, rinsed with deionized water, and autoclaved; then each sterilized rock fragment was immersed in BG11 liquid medium on a Petri dish and a small aliquot of strain GR2 pure culture was added. The rock-containing Petri dishes were incubated under the culture conditions used to cultivate strain GR2, as reported above. After a week of incubation, each rock fragment was transferred to another Petri dish containing BG11 liquid medium in the same culture conditions; this operation was repeated once to eliminate filaments of strain GR2 that were not attached to the rock. Different rock fragments, obtained in this way, were observed with an inverted microscope Leica DMI4000 B (Wetzlar, Germany), equipped with a digital image acquisition system.

Phycobiliprotein analysis

Culture aliquots of the three strains (three replicates for each strain) were ground in a mortar with liquid nitrogen and phycobiliproteins (PBPs) were extracted by adding a phosphate buffer (0.01 M NaH_2PO_4, 0.15 M NaCl, pH 7) to the homogenates and keeping them in the darkness, at 4°C, for 24h. The extract spectra and absorbances were analysed with a DU530 Beckman Coulter spectrophotometer (Fullerton, California, USA). Absorbance values at 562 nm (phycoerythrin), 615 nm (C-phycocyanin), and 652 nm (allophycocyanin) were recorded and used to calculate the concentration of PBPs following the formulae proposed by Bennett & Bogorad (1973).

RESULTS

Phylogenetic results

Phylogenetic reconstruction based on the 16S rRNA gene (Figs 1 and S1 (see doi/10.7872/crya/v38.iss4.2017.Suppl.Mat.)) highlighted fifteen well-supported clades inside the family Leptolyngbyaceae, eleven of which corresponding to previously described genera: *Thermoleptolyngbya* Sciuto & Moro, *Oculatella* Zammit *et al.*, *Trichocoleus* Anagnostidis, *Leptolyngbya* Anagnostidis & Komárek, *Plectolyngbya* Taton *et al.*, *Alkalinema* Vaz *et al.*, *Phormidesmis* Turicchia *et al.*, *Kovacikia* Miscoe *et al.*, *Stenomitos* Miscoe & Johansen, *Pantanalinema* Vaz *et al.*, *Halomicronema* Abed *et al.*, and *Nodosilinea* Perkerson & Casamatta. Of the four

remaining clusters, two were made up by cyanobacteria isolated from Antarctica; the first one included strains identified as *Leptolyngbya frigida* (Fritsch) Anagnostidis & Komárek, and it was therefore named the "*Leptolyngbya frigida*" clade, the second one contained strains attributed to *Leptolyngbya antarctica* (West & G.S.West) Anagnostidis & Komárek, and it was therefore tagged as the "*Leptolyngbya antarctica*" clade.

The other two lineages were clearly distinct from the other genera of the family Leptolyngbyaceae with high statistical support; they were named clades A and B.

Clade A included the sequences of strains GR4 and GR13 and 14 other sequences of cyanobacteria detected during environmental surveys (Fig. 1); a few of these strains were attributed to the genus *Leptolyngbya*, but the majority of them were just labelled as "uncultured cyanobacterium". Most of the cyanobacteria included in clade A were isolated from Antarctica, and a few were from the Arctic and alpine environments (Table 1, Fig. 1). The 16S rRNA gene sequences forming clade A ranged from 95.83% to 100% identity, based on the alignment used for the phylogenetic analyses (Fig. S2, see doi/10.7872/crya/v38.iss4.2017.Suppl.Mat.). The 16S rRNA sequences of strains GR4 and GR13 were 98.70% similar based on the longest possible alignment between them (1383 positions) and 98.65% based on an alignment of 1119 positions, including other focus taxa (Fig. S5, see doi/10.7872/crya/v38.iss4.2017.Suppl.Mat.).

Clade B included the sequence of strain GR2 and 16 other sequences of cyanobacteria, mainly detected during environmental studies. Many of the cyanobacterial strains belonging to clade B were not attributed to known taxa, while others were tentatively identified as various genera: *Heteroleibleinia* (Geitler) Hoffmann, *Leptolyngbya*, *Phormidesmis*, *Plectonema* Thuret ex Gomont, *Pseudanabaena* Lauterborn, and *Pseudophormidium* (Forti) Anagnostidis & Komárek. More than half of the clade B strains were isolated from Antarctica (Table 2, Fig. 1). Based on the alignment used for the phylogenetic analyses, the 16S rRNA gene sequences of clade B ranged from 95.24% to 100% similarity (Fig. S2, see doi/10.7872/crya/v38.iss4.2017.Suppl.Mat.). Strain GR2 had the highest 16S rRNA sequence identities (97.84-98.27%) with three uncultured strains (clone BGC-Fr054, isolate OUT 00162, strain QSSC8cya), with *Phormidesmis priestleyi* ANT.LPR2.6 (98.56%), and with *Heteroleibleinia fontana* UCFM_HF (97.98%). *H. fontana* UCFM_HF and *P. priestleyi* ANT.LPR2.6 shared a sequence identity of 98.27%.

The alignment used for phylogenetic analyses was constrained in length because the sequence of *H. fontana* UCFM_HF (KF264596) was only 694 bp long. Strain GR2 and *P. priestleyi* ANT.LPR2.6 had an identity of 97.32% on the longest alignment that could be obtained between their 16S rRNA sequences (1343 positions). Focusing on the sequences of GR2, *H. fontana* UCFM_HF, and *P. priestleyi* ANT.LPR2.6, the fragment of 16S rRNA common to all the three strains corresponded to the central part of the alignment achievable between the sequences of strain GR2 and *P. priestleyi* ANT.LPR2.6 (Fig. S6, see doi/10.7872/crya/v38.iss4.2017.Suppl.Mat.). Inside this alignment, 26 nucleotide substitutions were in the portion common only to strain GR2 and *P. priestleyi* ANT.LPR2.6, and 17 were in the portion common to all the three strains. Of the nucleotide differences falling in the common portion of the alignment, strain GR2 and *H. fontana* UCFM_HF had identical nucleotides in 3 positions, strain GR2 and *P. priestleyi* ANT.LPR2.6 showed identical nucleotides in 7 positions, and *H. fontana* UCFM_HF and *P. priestleyi* ANT.LPR2.6 had identical nucleotides in 5 positions. In the 2 remaining positions different nucleotides were observed among the three strains (Fig. S6).

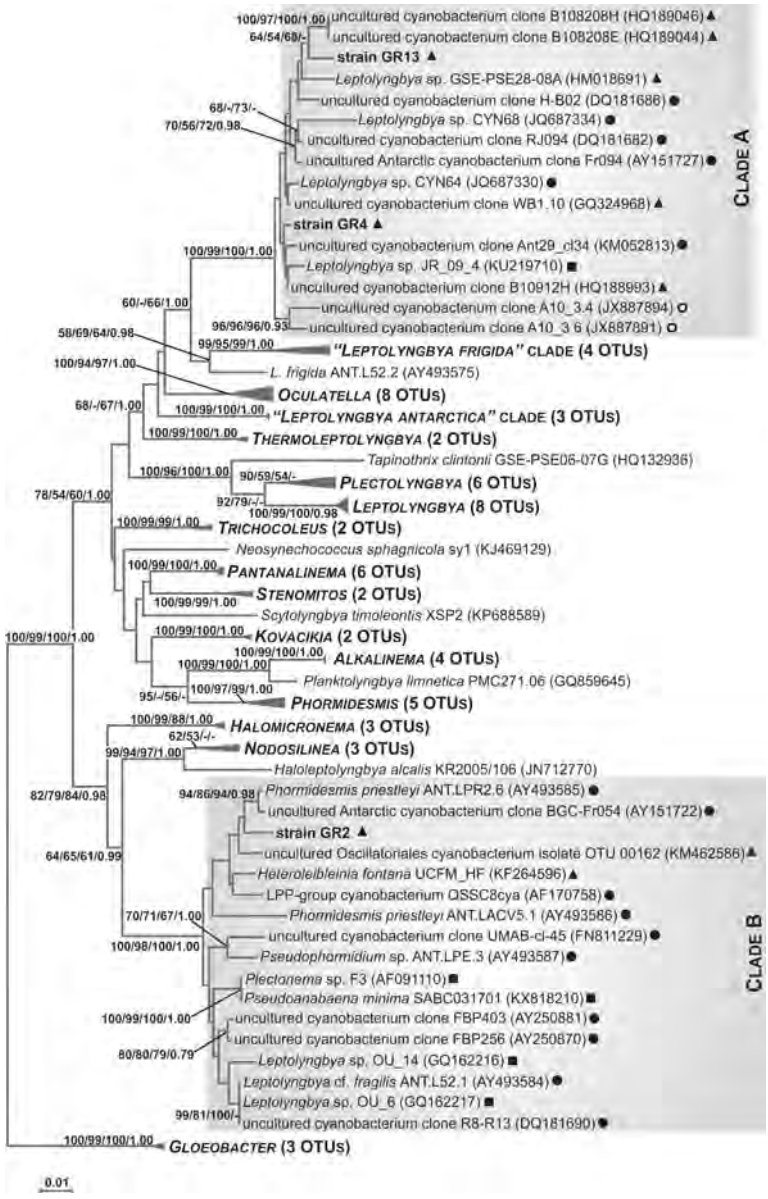

Fig. 1. Phylogenetic reconstruction of Leptolyngbyaceae based on 16S rRNA gene analyses. The NJ topology is depicted and the numbers associated with nodes indicate support values for NJ, MP, ML, and BI analyses, respectively. Only bootstrap supports ≥ 50% and posterior probabilities ≥ 0.70 are reported. Values for nodes that obtained support in only one of the performed phylogenetic analyses were omitted. Horizontal bar represents expected number of nucleotide substitutions per site. Clades A and B are highlighted by gray boxes; known genera, as well as the "*Leptolyngbya frigida*" and "*Leptolyngbya Antarctica*" clades, are represented by grey triangles with the number of considered OTUs reported in parentheses. Inside clades A and B, a symbol near each considered strain indicates if it was isolated from a mountain habitat (black triangle), from Antarctica (black circle), from the Arctic (white circle), or from a different environment (black square). The extended 16S rRNA tree is depicted in Fig. S1.

Table 1. Strains belonging to Clade A in the 16S rDNA phylogenetic reconstruction, besides strains GR4 and GR13. For each strain, the INSD accession number of the 16S rDNA gene sequence, the former/provisional identification of the strain, the collection site, ecological data, and literature reference are reported. A dash denotes that no data are available

Accession number	*Identified as*	*Collection site*	*Ecological data*	*References*
AY151727	uncultured Antarctic cyanobacterium clone Fr094	Lake Fryxell, Taylor Valley, Southern Victoria Land, Antarctica	from a shallow moat area in a brackish and meromictic lake	Taton *et al.*, 2003
DQ181682	uncultured cyanobacterium clone RJ094	Lake Reid, Larsemann Hills, East Antarctica	–	Taton *et al.*, 2006a
DQ181686	uncultured cyanobacterium clone H-B02	Lake Heart, Larsemann Hills, East Antarctica	–	Taton *et al.*, 2006a
GQ324968	uncultured cyanobacterium clone WB1.10	Harz Mountains, Westerhoefer Creek, Germany	freshwater, from biofilm on rock surface in karstwater stream	Arp *et al.*, 2010
HM018691	*Leptolyngbya* sp. GSE-PSE28-08A	Grand Staircase-Escalante National Monument, Utah, USA	from subaerial wet wall, mountain environment	Perkerson *et al.*, 2011
HQ188993	uncultured cyanobacterium clone B10912H	Annapurna Range, Nepal	from alpine soil, subnival, 0-4 cm depth	Schmidt *et al.*, 2011
HQ189044	uncultured cyanobacterium clone B108208E	Annapurna Range, Nepal	from alpine soil, subnival, 0-4 cm depth	Schmidt *et al.*, 2011
HQ189046	uncultured cyanobacterium clone B108208H	Annapurna Range, Nepal	from alpine soil, subnival, 0-4 cm depth	Schmidt *et al.*, 2011
JQ687330	*Leptolyngbya* sp. CYN64	Pyramid Trough, Southern Victoria Land, Antarctica	benthic mat, shallow melt-water pond ("Cleopatra pond")	Martineau *et al.*, 2013
JQ687334	*Leptolyngbya* sp. CYN68	Pyramid Trough, Southern Victoria Land, Antarctica	benthic mat, shallow melt-water pond ("Egypt pond")	Martineau *et al.*, 2013
JX887891	uncultured cyanobacterium clone A10_3.6	Northern Baffin Island, Cape Hatt, Arctic	freshwater microbial mat	Kleinteich *et al.*, 2013
JX887894	uncultured cyanobacterium clone A10_3.4	Northern Baffin Island, Cape Hatt, Arctic	freshwater microbial mat	Kleinteich *et al.*, 2013
KM052813	uncultured cyanobacterium clone Ant29_cl34	Wright Valley, Antarctica	soil	Novis, unpublished
KU219710	*Leptolyngbya* sp. JR_09_4	–	epilithon in littoral of lake	Strunecky *et al.*, unpublished

Table 2. Strains belonging to Clade B in the 16S rDNA phylogenetic reconstruction, besides strain GR2. For each strain, the INSD accession number of the 16S rDNA gene sequence, the former/provisional identification of the strain, the collection site, ecological data, and literature reference are reported. A dash denotes that no data are available

Accession number	*Identified as*	*Isolated from*	*Ecological data*	*References*
AF091110	*Plectonema* sp. F3	Saint-Valéry-sur-Somme, Manche, France	marine, from Atlantic mediolittoral zone	Wilmotte, 1991; Turner, 1997
AF170758	LPP-group cyanobacterium QSSC8cya	Vestfold Hills, Eastern Antarctica	sublithic in quartz stones, non-halophilic, optimum growth at 15-20°C	Smith *et al.*, 2000
AY151722	uncultured Antarctic cyanobacterium clone BGC-Fr054	Lake Fryxell, Taylor Valley, Southern Victoria Land, Antarctica	from a shallow moat area in a brackish and meromictic lake	Taton *et al.*, 2003
AY250870	uncultured cyanobacterium clone FBP256	McMurdo dry valleys, Southern Victoria Land, Antarctica	in lichen-dominated cryptoendolithic community	De la Torre *et al.*, 2003
AY250881	uncultured cyanobacterium clone FBP403	McMurdo dry valleys, Southern Victoria Land, Antarctica	in lichen-dominated cryptoendolithic community	De la Torre *et al.*, 2003
AY493584	*Leptolyngbya* cf. *fragilis* ANT.L52.1	Larsemann Hills, Prydz Bay region, Eastern Antarctica	lake/pond	Taton *et al.*, 2006b
AY493585	*Phormidesmis priestleyi* ANT.LPR2.6	Antarctica	lake/pond	Taton *et al.*, 2006b
AY493586	*Phormidesmis priestleyi* ANT.LACV5.1	Antarctica	lake/pond	Taton *et al.*, 2006b
AY493587	*Pseudophormidium* sp. ANT.LPE.3	Antarctica	lake/pond	Taton *et al.*, 2006b
DQ181690	uncultured cyanobacterium clone R8-R13	Lake Rauer, Rauer Islands, East Antarctica	shallow, hyposaline lake; strain isolated from the uppermost part of the mat, collected in the littoral part of the lake	Taton *et al.*, 2006a
FN811229	uncultured cyanobacterium clone UMAB-cl-45	Mars Oasis, Alexander Island, Antarctica	on grey sedimentary rocks in the maritime/ continental transitional zone	Chong *et al.*, 2012
GQ162216	*Leptolyngbya* sp. OU_14	Beer, Devon, United Kingdom	epilithic on a cliff surface made of Cretaceous nodular chalk limestone, submerged in seawater during high tide	Olsson-Francis *et al.*, 2010
GQ162217	*Leptolyngbya* sp. OU_6	Beer, Devon, United Kingdom	epilithic on a cliff surface made of Cretaceous nodular chalk limestone, submerged in seawater during high tide	Olsson-Francis *et al.*, 2010
KF264596	*Heteroleibleinia fontana* UCFM_HF	Kaituna river and its tributaries, Banks Peninsula, New Zealand	epilithic, mainly in unshaded second order and partly shaded third order tributary streams	Merican, 2013
KM462586	uncultured Oscillatoriales cyanobacterium isolate OTU 00162	Koolau Mountain Range, Oahu, Hawaii, USA	environmental air sample ARS08519	Sherwood *et al.*, 2014
KX818210	*Pseudoanabaena minima* SABC031701	Tralee, Ireland	–	Katie *et al.*, unpublished

Only one ribosomal operon, with both the $tRNA^{Ile}$ and $tRNA^{Ala}$ genes inside the ITS region, was recovered for each of the strains GR2, GR4, and GR13. Few 16S-23S ITS sequences of the other cyanobacteria belonging to clades A and B in the 16S rRNA phylogenetic reconstruction could be analyzed, because for many strains sequences of this locus were not available or they were too short. Also, fewer members of known genera were included in the phylogenetic analyses based on the ITS region, given the higher variability of this locus and the consequent difficulty to obtain reliable alignments with distantly related taxa. The phylogenetic tree based on the 16S-23S ITS is depicted in Fig. 2 and allowed the detection of ten well-supported clades, seven of which corresponding to known lineages (*Alkalinema, Phormidesmis*, *Kovacikia*, *Oculatella*, *Trichocoleus*, *Plectolynbgya*, and *Leptolyngbya*). As found with the 16S rRNA analysis, the "*Leptolyngbya frigida*" clade had high statistical support, as did clades A and B, which were again clearly distinct from the other known taxa inside the family Leptolyngbyaceae. The well-supported group formed by *Haloleptolyngbya alcalis* KR2005/106 and a representative of the genus *Nodosilinea* was used to root the tree.

16S-23S ITS secondary structure data

Hypothetical secondary structures of the 16S-23S ITS region (containing both tRNA genes) were estimated for the D1-D1' domain (Figs 3 and 6), boxB domain (Figs 4 and 7), and V3 domain (Figs 5 and 8) of the cyanobacterial strains belonging to clades A and B in the ITS region tree.

Clade A: Only one hypothetical secondary structure was generated by the program RNAstructure for the D1-D1' domain of each of the strains belonging to clade A. The obtained structures are reported in Fig. 3 and described in detail in Table 3; they showed a variable length ranging from 63 to 85 residues. All the inferred structures were comparable in the first portion, which was composed by a 5-residue basal stem (GACCU-AGGUC) followed by a 8 residue right bulge (CAYCCCAA). The remaining part of the D1-D1' structure varied greatly among the clade A strains, with similarities found between strain pairs. In particular, the D1-D1' helices of strains GR4 and GR13 showed the same length (85 residues) and had several features in common (Fig. 3, Table 3); in the terminal part one compensatory base change (CBC, i.e. a nucleotide substitution in both the side of a paired region in order to keep the structure) and two hemi-compensatory base changes (hCBCs, i.e. nucleotide substitutions in one of the sides of a paired region in order to keep the structure) were observed between the structures of the two organisms (Fig. 3).

Also for the boxB domain, only one hypothetical secondary structure was predicted by the program RNAstructure for each strain of the clade A. The obtained structures are represented in Fig. 4 and thoroughly described in Table 3; they ranged in size from 35 to 61 residues. The first part of the boxB helix was identical for all the investigated strains, while the remaining portion varied greatly (indicated by two dotted line arrows in Fig. 4). In the basal part of the boxB helix, common to all the considered strains, one hCBC was observed between the structures of strains GR4 and GR13 (Fig. 4).

The hypothetical secondary structures of the V3 domain could be predicted only for four strains included in clade A, since for the other three strains the available 16S-23S ITS sequences were too short. Only one V3 secondary structure was generated by the program RNAstructure for each of the considered strains. The obtained structures (Fig. 5) ranged in size from 59 to 61 residues and are described in detail in Table 3. The major part of the predicted V3 secondary helices was congruent among the investigated strains. In the central portion, one CBC and four hCBCs were observed between the structures of strains GR4 and GR13 (Fig. 5).

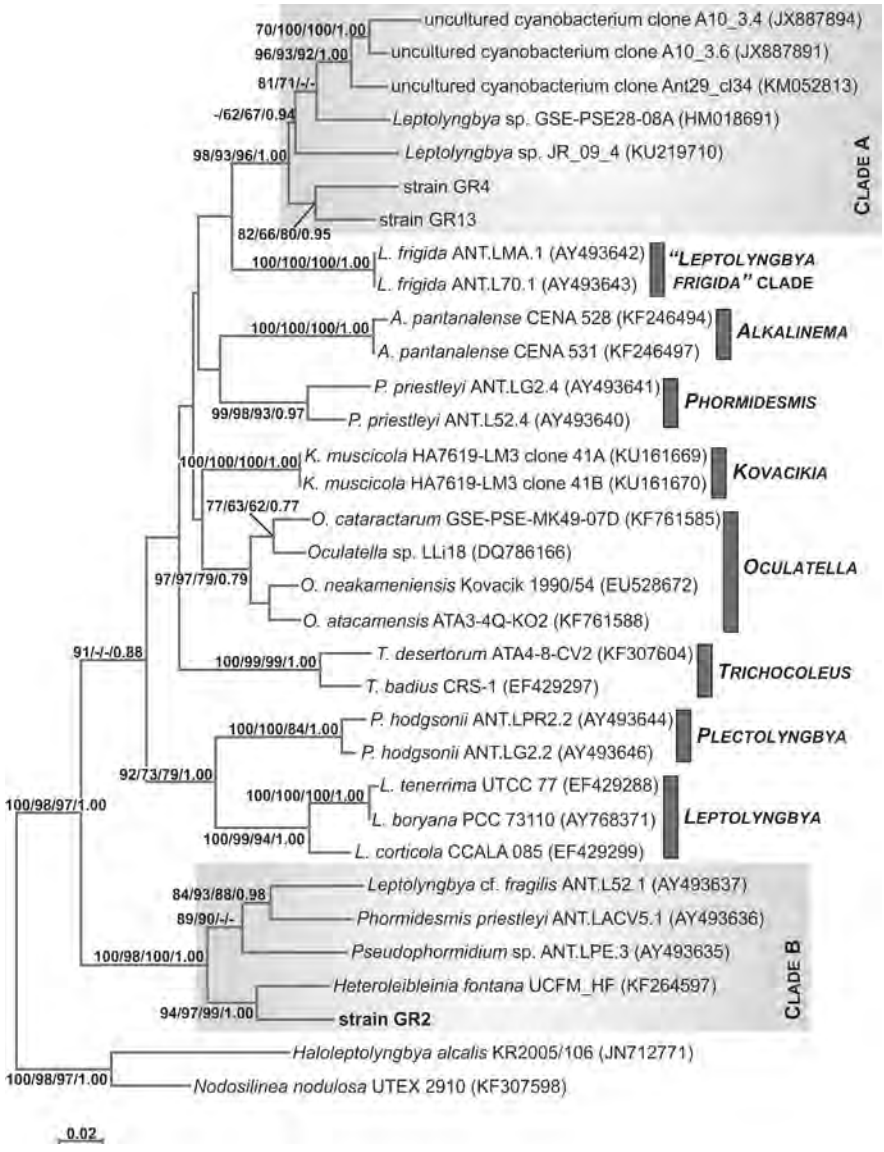

Fig. 2. Phylogenetic reconstruction of Leptolyngbyaceae based on the 16S-23S ITS region analyses. The NJ topology is depicted and the numbers associated with nodes indicate support values for NJ, MP, ML, and BI analyses, respectively. Only bootstrap supports ≥ 50% and posterior probabilities ≥ 0.70 are reported. Values for nodes that obtained support in only one of the performed phylogenetic analyses were omitted. Horizontal bar represents expected number of nucleotide substitutions per site. Genera are indicated by vertical bars and clades A and B are highlighted by gray boxes.

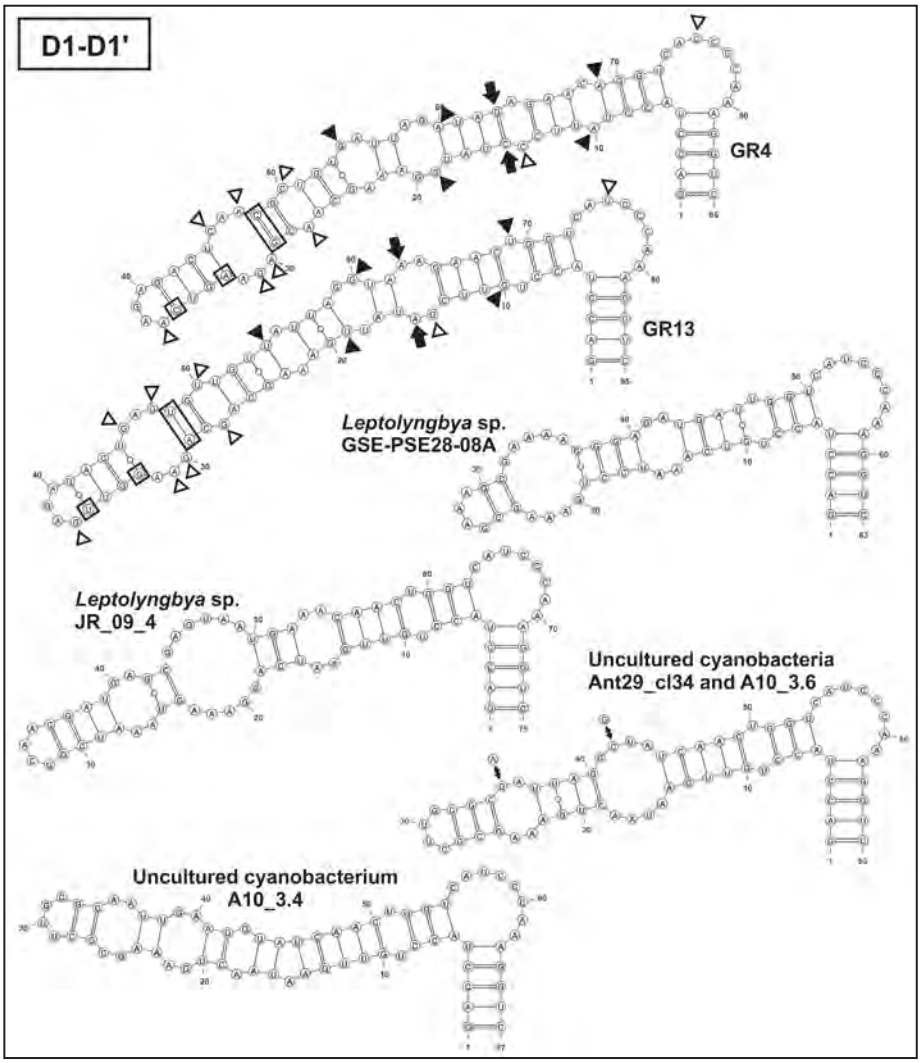

Fig. 3. Hypothetical secondary structures of the 16S-23S ITS region D1-D1' helix for the cyanobacterial strains forming clade A in the 16S-23S ITS phylogenetic reconstruction. In paired regions, A-U pairings are represented with a single line, G-C pairings with a double line, and unconventional pairings with a line interrupted by a circle. Nucleotide substitutions for a given structure are illustrated by double-headed black arrows plus circles inscribing nucleotide symbols near the interested nucleotide positions. Nucleotide changes between strains GR4 and GR13 are indicated as follows: white arrow heads = single nucleotide changes not causing a change in the structure); black arrow heads = single nucleotide changes causing a change in the structure; black arrow pairs = pairs of nucleotide changes causing a change in the structure; black squares = hCBCs; black rectangles = CBCs.

Table 3. Detailed descriptions of the ITS structures for the strains belonging to clade A. The total length of each helix is given in parentheses near the cyanobacterial strain designation; the residues involved are reported in parentheses near the corresponding secondary structures. For three clade A cyanobacteria (clone A10_3.4, clone A10_3.6, clone Ant29_cl34) the V3 helix was not obtained

	STRAIN DESIGNATION	
D1-D1'	GR4 (85 residues)	5-residue basal stem (GACCU-AGGUC) + 8-residue right bulge (CACCCCAA) + 4-residue stem region (ACCU-AGGU) + 2-residue symmetrical internal loop (A-C) + 3-residue stem region (UUC-GAA) + 2-residue symmetrical internal loop (C-A) + 4-residue stem region (CUAU-AUAG) + 4-residue symmetrical internal loop (GG-AG) + 2-residue stem region (AA-UU) + 3-residue asymmetrical internal loop (A-GA) + 3-residue stem region (GCA-UGU) + 2-residue symmetrical internal loop (A-C) + 2-residue stem region (CG-CG) + 3-residue symmetrical internal loop (AGA-CAA) + 4-residue stem region (AGUC-GACU) + 4-residue terminal hairpin (AAGA)
	GR13 (85 residues)	5-residue basal stem (GACCU-AGGUC) + 8-residue right bulge (CAUCCCAA) + 3-residue stem region (ACC-GGU) + 2-residue-symmetrical internal loop (U-U) + 4-residue stem region (GUUC-GAAC) + 4-residue symmetrical internal loop (GA-AA) + 2-residue stem region (UA-UA) + 3-residue asymmetrical internal loop (U-GG) + 3-residue stem region (UGA-UUA) + 2-residue symmetrical internal loop (A-A) + 4-residue stem region (AGCA-UGUU) + 2-residue symmetrical internal loop (G-U) + 2-residue stem region (CA-UG) + 3-residue symmetrical internal loop (GAA-GAG) + 4-residue stem region (GGUU-GACU) + 4-residue terminal hairpin (GAGA)
	Leptolyngbya sp. GSE-PSE28-08A (63 residues)	5-residue basal stem (GACCU-AGGUC) + 8-residue right bulge (CAUCCCAA) + 3-residue stem region (ACC-GGU) + 2-residue-symmetrical internal loop (U-U) + 4-residue stem region (GUCA-UGAU) + 4-residue symmetrical internal loop (AA-GA) + 4-residue stem region (UCCU-GGGA) + 9-residue asymmetrical internal loop (GAAA-GAAAA) + 2-residue stem region (GC-GC) + 4-residue terminal hairpin (GAAA)
	Leptolyngbya sp. JR_09_4 (75 residues)	5-residue basal stem (GACCU-AGGUC) + 8-residue right bulge (CAUCCCAA) + 3-residue stem region (ACC-GGU) + 2-residue-symmetrical internal loop (U-U) + 4-residue stem region (GUUG-CAAC) + 4-residue symmetrical internal loop (AA-AA) + 3-residue stem region (UCA-UGA) + 11-residue asymmetrical internal loop (GGAAA-GAGUAA) + 2-residue stem region (GU-GC) + 4-residue symmetrical internal loop (AA-GA) + 4-residue stem region (AUCG-CGAU) + 4-residue terminal hairpin (GCAA)
	uncultured cyanobacterium clone A10_3.4 (67 residues)	5-residue basal stem (GACCU-AGGUC) + 8-residue right bulge (CAUCCCAA) + 3-residue stem region (ACC-GGU) + 2-residue-symmetrical internal loop (U-U) + 5-residue stem region (GUUGA-UCAAC) + single base left bulge (A) + 2-residue stem region (UA-UA) + 2-residue symmetrical internal loop (A-G) + 2-residue stem region (CU-AG) + 4-residue symmetrical internal loop (GA-GA) + 2-residue stem region (AA-UU) + 4-residue symmetrical internal loop (GC-AA) + 2-residue stem region (GC-GC) + 4-residue terminal hairpin (UUGC)
	uncultured cyanobacterium clone A10_3.6 (66 residues)	5-residue basal stem (GACCU-AGGUC) + 8-residue right bulge (CAUCCCAA) + 3-residue stem region (ACC-GGU) + 2-residue-symmetrical internal loop (U-U) + 5-residue stem region (GUUGA-UCAAC) + 8-residue symmetrical internal loop (AUAA-GGUA) + 4-residue stem region (CUGA-UUAG) + 4-residue symmetrical internal loop (AA-AA) + 3-residue stem region (GCG-CGC) + 4-residue terminal hairpin (CUUG)
	uncultured cyanobacterium clone Ant29_cl34 (66 residues)	5-residue basal stem (GACCU-AGGUC) + 8-residue right bulge (CAUCCCAA) + 3-residue stem region (ACC-GGU) + 2-residue-symmetrical internal loop (U-U) + 5-residue stem region (GUUGA-UCAAC) + 8-residue symmetrical internal loop (AUAA-GCUA) + 4-residue stem region (CUGA-UUAG) + 4-residue symmetrical internal loop (AA-GA) + 3-residue stem region (GCG-CGC) + 4-residue terminal hairpin (CUUG)

boxB	GR4 (52 residues)	5-residue basal stem (CAGCA-UGCUG) + 3-residue asymmetrical internal loop (A-CC) + 2-residue stem (CU-AG) + 3-residue asymmetrical internal loop (GA-G) + 5-residue stem region (UCUAG-CUAGA) + 3-residue asymmetrical internal loop (C-CU) + 4-residue stem region (GAAG-CUUC) + 2-residue symmetrical internal loop (A-C) + 2-residue stem region (UU-AA) + 5-residue terminal hairpin (CAAUU)
	GR13 (46 residues)	5-residue basal stem (CAGCA-UGCUG) + 3-residue asymmetrical internal loop (A-CC) + 2-residue stem (CU-AG) + 3-residue asymmetrical internal loop (UG-G) + 11-residue stem region (UUUAAUUUAUC-GAUAAAUUAGA) + 4-residue terminal hairpin (AAGG)
	Leptolyngbya sp. GSE-PSE28-08A (51 residues)	5-residue basal stem (CAGCA-UGCUG) + 3-residue asymmetrical internal loop (A-CC) + 2-residue stem (CU-AG) + 3-residue asymmetrical internal loop (GA-G) + 5-residue stem region (UCUAG-CUAGA) + 7-residue asymmetrical internal loop (AG-AAUAG) + 4-residue stem region (GAUA-UAUC) + 6-residue terminal hairpin (UUAAUU)
	Leptolyngbya sp. JR_09_4 (35 residues)	5-residue basal stem (CAGCA-UGCUG) + 3-residue asymmetrical internal loop (A-CC) + 2-residue stem (CU-AG) + 3-residue asymmetrical internal loop (UA-G) + 5-residue stem region (UCUAG-CUAGA) + 5-residue terminal hairpin (AUGAA)
	uncultured cyanobacterium clone A10_3.4 (61 residues)	5-residue basal stem (CAGCA-UGCUG) + 3-residue asymmetrical internal loop (A-CC) + 2-residue stem (CU-AG) + 3-residue asymmetrical internal loop (UA-G) + 4-residue stem region (UCUA-UAGA) + 5-residue asymmetrical internal loop (GA-AAA) + 10-residue stem region (UAUUCUCAAG-UUUGGGAAUA) + 8-residue terminal hairpin (GGAUUGAG)
	uncultured cyanobacterium clone A10_3.6 (61 residues)	5-residue basal stem (CAGCA-UGCUG) + 3-residue asymmetrical internal loop (A-CC) + 2-residue stem (CU-AG) + 3-residue asymmetrical internal loop (UA-G) + 4-residue stem region (UCUA-UAGA) + 5-residue asymmetrical internal loop (GA-AGA) + 10-residue stem region (UAUUCUCAAG-UUUGGGAAUA) + 8-residue terminal hairpin (GGAUUGAG)
	uncultured cyanobacterium clone Ant29_cl34 (51 residues)	5-residue basal stem (CAGCA-UGCUG) + 3-residue asymmetrical internal loop (A-CC) + 2-residue stem (CU-AG) + 3-residue asymmetrical internal loop (GG-G) + 5-residue stem region (UCUAG-CUAGA) + 5-residue asymmetrical internal loop (C-UCAA) + 5-residue stem region (GGAUA-UAUCU) + 6-residue terminal hairpin (UUAGAU)
V3	GR4 (59 residues)	4-residue basal stem (UGUC-GACA) + 4-residue asymmetrical internal loop (A-ACA) + 4-residue stem region (GGUA-UAUC) + 4-residue asymmetrical internal loop (G-AAG) + 12-residue stem region (UCGUUAAUUGAG-CUCAGUUAACGA) + 2-residue symmetrical internal loop (A-C) + 2-residue stem region (GU-GC) + 5-residue terminal hairpin (GAUUA)
	GR13 (59 residues)	4-residue basal stem (UGUC-GACA) + 4-residue asymmetrical internal loop (A-ACA) + 4-residue stem region (GGUA-UAUC) + 4-residue asymmetrical internal loop (G-AAG) + 14-residue stem region (UUGUUAGUUGAGAG-UUCUCGACUAACGA) + 7-residue terminal hairpin (CGAUGAA)
	Leptolyngbya sp. GSE-PSE28-08A (61 residues)	4-residue basal stem (UGUC-GACA) + 4-residue asymmetrical internal loop (A-AUA) + 4-residue stem region (GGUA-UAUC) + 4-residue asymmetrical internal loop (G-AGA) + 12-residue stem region (UUGUCAUUUGGG-CCCGAGUGACAG) + 3-residue asymmetrical internal loop (A-CC) + 2-residue stem region (CU-AG) + 6-residue terminal hairpin (UUGAUU)
	Leptolyngbya sp. JR_09_4 (60 residues)	4-residue basal stem (UGUC-GACA) + 4-residue asymmetrical internal loop (A-ACA) + 4-residue stem region (GGUA-UAUC) + 4-residue asymmetrical internal loop (G-AUG) + 12-residue stem region (UCAAUGAUUGGG-CCCAGUUGUUGA) + 3-residue asymmetrical internal loop (A-CC) + 3-residue stem region (CUA-UAG) + 3-residue terminal hairpin (GAU)

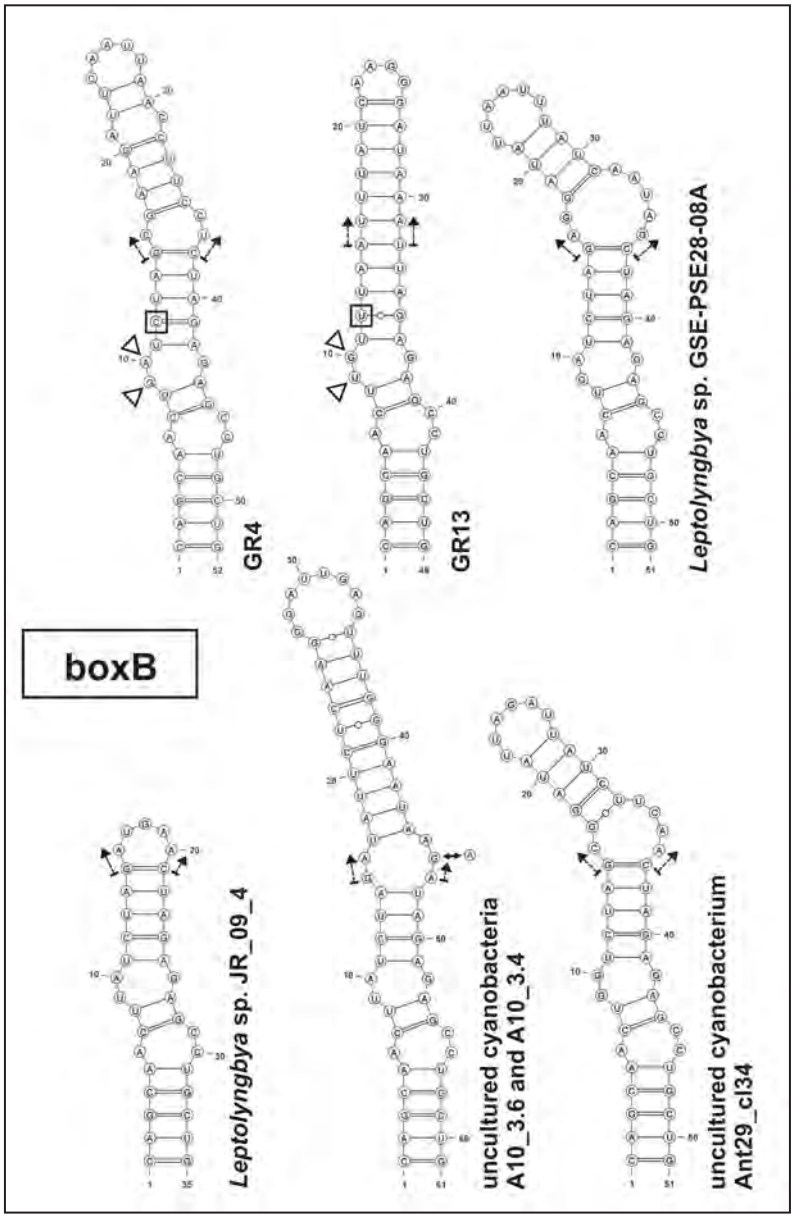

Fig. 4. Hypothetical secondary structures of the 16S-23S ITS region boxB helix for the cyanobacterial strains forming clade A in the 16S-23S ITS phylogenetic reconstruction. In paired regions, A-U pairings are represented with a single line, G-C pairings with a double line, and unconventional pairings with a line interrupted by a circle. Nucleotide substitutions for a given structure are illustrated by double-headed black arrows plus circles inscribing nucleotide symbols near the interested nucleotide positions. The start of boxB helix terminal portion that varies among the considered strains is highlighted by two dotted line arrows. In the boxB helix portion common to all the considered strains, nucleotide changes between strains GR4 and GR13 are indicated as follows: white arrow heads = single nucleotide changes not causing a change in the structure; black squares = hCBCs.

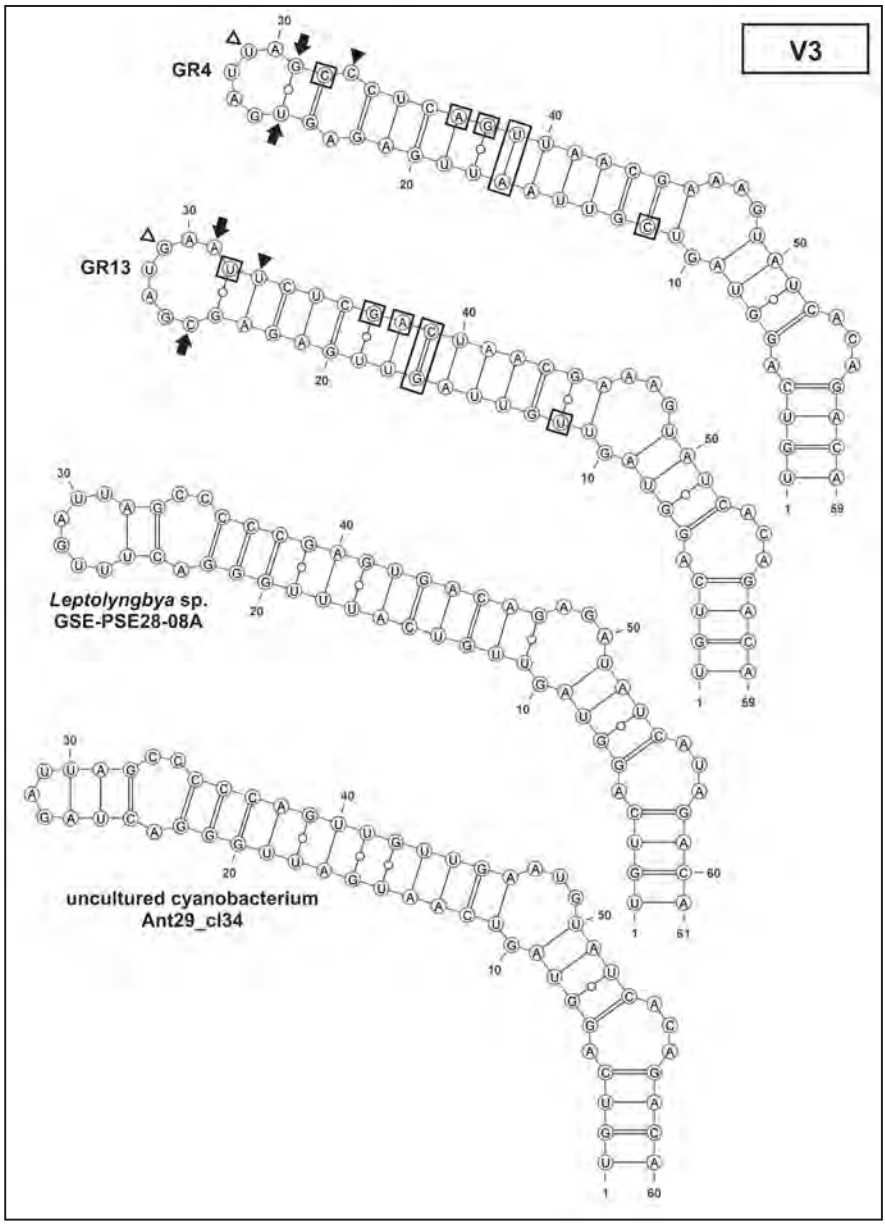

Fig. 5. Hypothetical secondary structures of the 16S-23S ITS region V3 helix for the cyanobacterial strains forming clade A in the 16S-23S ITS phylogenetic reconstruction. In paired regions, A-U pairings are represented with a single line, G-C pairings with a double line, and unconventional pairings with a line interrupted by a circle. Nucleotide substitutions for a given structure are illustrated by double-headed black arrows plus circles inscribing nucleotide symbols near the interested nucleotide positions. Nucleotide changes between strains GR4 and GR13 are indicated as follows: white arrow heads = single nucleotide changes not causing a change in the structure); black arrow heads = single nucleotide changes causing a change in the structure; black arrow pairs = pairs of nucleotide changes causing a change in the structure; black squares = hCBCs; black rectangles = CBCs.

Since in both the 16S rRNA and 16S-23S ITS region trees clade A was sister taxon to "*Leptolyngbya frigida*" clade, the ITS region secondary structures of this lineage were also investigated. The two *L. frigida* strains (ANT.LMA.1 and AY493643) included in the ITS phylogenetic reconstruction had identical ITS region sequences. Only one structure was generated by the program RNAstructure for each of the considered ITS region domains of the "*Leptolyngbya frigida*" clade; they are depicted in Fig. S7 (see doi/10.7872/crya/v38.iss4.2017.Suppl.Mat.). The D1-D1' helix was 75 residues long; it was composed as follows: 5-residue basal stem (GACCU-AGGUC) + 10-residue asymmetrical internal loop (A-CCAUCCCAA) + 2-residue stem region + 2-residue symmetrical internal loop + 4-residue stem region + 4-residue symmetrical internal loop + 4-residue stem region + 6-residue symmetrical internal loop + single base right bulge (U) + 2-residue stem region + 4-residue symmetrical internal loop + 4-residue stem region + 4-residue terminal hairpin loop. The box B secondary structure of "*L. frigida*" clade was 39 residues long; it appeared as a straight helix, interrupted by two 2-residue symmetrical internal loops and with a 5-residue terminal hairpin loop. The V3 helix of "*L. frigida*" clade was 94 residues long; it was composed as follows: 4-residue basal stem (UGUC-GACA) + 3-residue asymmetrical internal loop (AG-A) + 5-residue stem region + 3-residue left bulge (AAC) + 15-residue stem region + 14-residue symmetrical internal loop + 5-residue stem region + 6-residue symmetrical internal loop + 3-residue stem region + 4-residue terminal hairpin loop.

Clade B: The program RNAstructure produced one hypothetical D1-D1' secondary structure for strain GR2, *Phormidesmis priestleyi* ANT.LACV5.1, and *Leptolyngbya* cf. *fragilis* ANT.L52.1, and three hypothetical structures for *Heteroleibleinia fontana* UCFM_HF and *Pseudophormidium* sp. ANT.LPE.3; in the second case the hypothetical structure with the lowest free energy was chosen. The obtained secondary structures are depicted in Fig. 6 and thoroughly described in Table 4. All the helices (63-65 residues long) were characterized by the same basal stem structure of 5 residues (GACCU-AGGUC), except for *H. fontana* UCFM_HF that showed a nucleotide substitution causing a shorter basal stem (Fig. 6). Also for the remaining part of the helix, *H. fontana* UCFM_HF had the most different structure, whereas the structures of all the other strains of clade A were more homogeneous among them, with differences in the length of the three last internal stems and of the terminal hairpin loop (Fig. 6, Table 4). The final part of *H. fontana* UCFM_HF helix was identical to those of strains GR2 and ANT.LPE.3 (Fig. 6, Table 4).

Only one hypothetical secondary structure was generated by the program RNAstructure for the boxB domain of each of the strains forming clade A; they are illustrated in Fig. 7 and described in detail in Table 4. The boxB hypothetical structures had a more variable length than those found for the D1-D1' helix, with a size ranging from 41 to 69 residues; strain GR2 and *H. fontana* UCFM_HF showed the longest boxB helices (Fig. 7). All the boxB helices of clade B strains shared a common structure in the first part, with strain *L.* cf. *fragilis* ANT.L52.1 showing some differences (Fig. 7, Table 4). The remaining part of the boxB helices mirrored the relationships found inside clade B with the 16S-23S ITS phylogenetic reconstruction; the structures of strain GR2 and *H. fontana* UCFM_HF were very similar, while the structures of the three remaining strains were more comparable among them, with a high similarity between the helices of strains ANT.LACV5.1 and ANT.L52.1 (Fig. 7, Table 4).

The 16S-23S ITS sequence of *Pseudophormidium* sp. ANT.LPE.3 was too short, resulting in a partial V3 domain; thus the V3 helix could not be predicted for

this strain. The program RNAstructure predicted only one V3 hypothetical secondary structure for each of the four remaining strains included in clade A; they are depicted in Fig. 8 and thoroughly described in Table 4. The obtained secondary structures mirrored the relationships highlighted by the 16S-23S ITS tree, with the helices of strain GR2 and *H. fontana* UCFM_HF sharing higher similarity between them than with each of the other two strains (*P. priestleyi* ANT.LACV5.1 and *L.* cf. *fragilis* ANT.L52.1). In particular, the V3 helices of strains ANT.LACV5.1 and ANT.L52.1 were longer (93-96 residues) than those of strains GR2 and UCFM_HF (77 residues) and also very different in structure, except for the same, very short, basal stem (Fig. 8, Table 4).

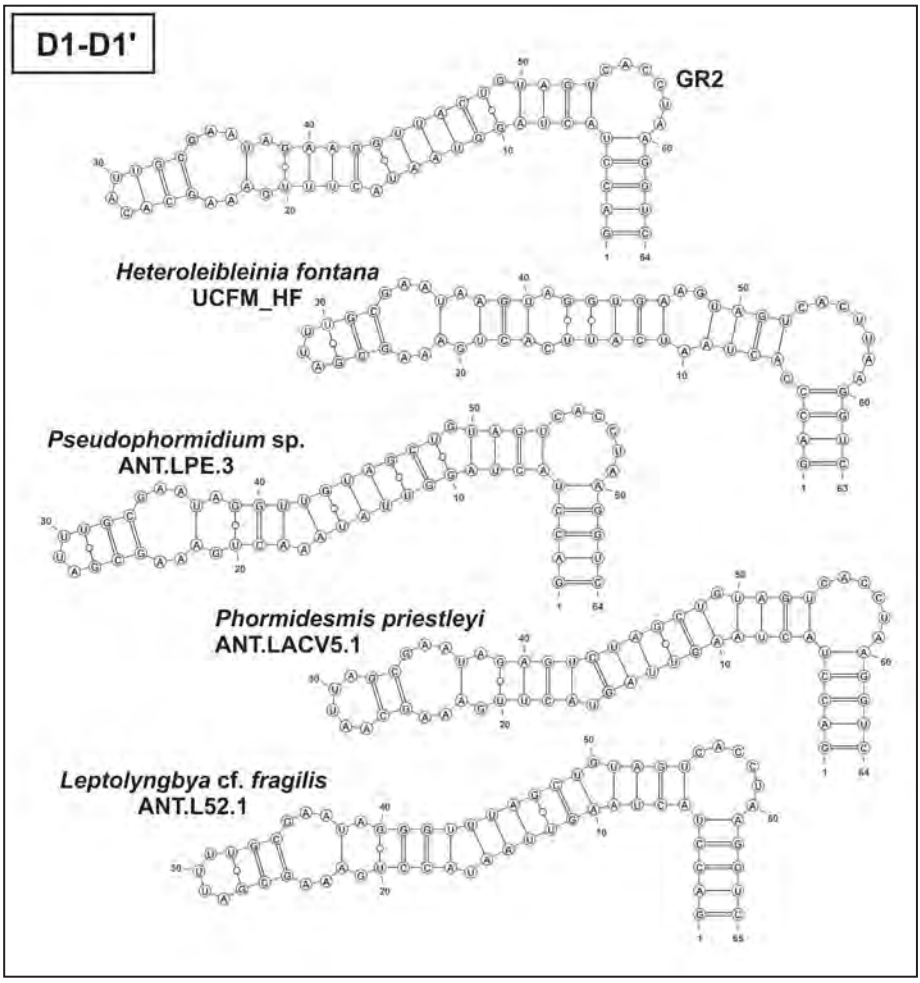

Fig. 6. Hypothetical secondary structures of the 16S-23S ITS region D1-D1' helix for the cyanobacterial strains forming clade B in the 16S-23S ITS phylogenetic reconstruction. In paired regions, A-U pairings are represented with a single line, G-C pairings with a double line, and unconventional pairings with a line interrupted by a circle.

Table 4. Detailed descriptions of the ITS structures for the strains belonging to clade B. The total length of each helix is given in parentheses near the cyanobacterial strain designation; the residues involved are reported in parentheses near the corresponding secondary structures. For *Pseudophormidium* sp. ANT.LPE.3 the V3 helix was not obtained

	STRAIN DESIGNATION	
D1-D1'	GR2 (64 residues)	5-residue basal stem (GACCU-AGGUC) + 6-residue right bulge (CACCUA) + 4-residue stem region (ACUA-UAGU) + single base right bulge (G) + 6-residue stem region (GGUAAU-GUUACU) + single base left bulge (A) + 4-residue stem region (CUUU-GAAG) + 2-residue symmetrical internal loop (G-A) + A-U pairing + 5-residue asymmetrical internal loop (AA-GAA) + 3-residue stem region (GCA-UGC) + 3-residue terminal hairpin loop (CAU)
	Heteroleibleinia fontana UCFM_HF (63 residues)	4-residue basal stem (GACC-GGUC) + 8-residue asymmetrical internal loop (C-CACUUAA) + 4-residue stem region (ACUA-UAGU) + 3-residue asymmetrical internal loop (A-AG) + 5-residue stem region (UCAUU-GGUGA) + 2-residue symmetrical internal loop (C-A) + 3-residue stem region (ACU-AGU) + 2-residue symmetrical internal loop (G-A) + A-U pairing + 5-residue asymmetrical internal loop (AA-GAA) + 3-residue stem region (GCG-UGC) + 3-residue terminal hairpin loop (AUU)
	Pseudophormidium sp. ANT.LPE.3 (64 residues)	5-residue basal stem (GACCU-AGGUC) + 6-residue right bulge (CACCUA) + 4-residue stem region (ACUA-UAGU) + single base right bulge (G) + 7-residue stem region (GGUUAUA-UGUAGCU) + single base left bulge (A) + 3-residue stem region (ACU-GGU) + 2-residue symmetrical internal loop (G-A) + A-U pairing + 5-residue asymmetrical internal loop (AA-GAA) + 3-residue stem region (GCG-UGC) + 3-residue terminal hairpin loop (AUU)
	Phormidesmis priestleyi ANT.LACV5.1 (64 residues)	5-residue basal stem (GACCU-AGGUC) + 6-residue right bulge (CACCUA) + 4-residue stem region (ACUA-UAGU) + single base right bulge (G) + 6-residue stem region (AGUUAG-CUAGCU) + single base left bulge (U) + 4-residue stem region (ACUU-GAGU) + 2-residue symmetrical internal loop (G-A) + A-U pairing + 5-residue asymmetrical internal loop (AA-GAA) + 2-residue stem region (GC-GC) + 5-residue terminal hairpin loop (AAUUA)
	Leptolyngbya cf. *fragilis* ANT.L52.1 (65 residues)	5-residue basal stem (GACCU-AGGUC) + 6-residue right bulge (CACCUA) + 4-residue stem region (ACUA-UAGU) + single base right bulge (G) + 6-residue stem region (AGUUAA-UUAGCU) + single base left bulge (U) + 4-residue stem region (ACCU-GGGU) + 2-residue symmetrical internal loop (G-A) + A-U pairing + 5-residue asymmetrical internal loop (AA-GAA) + 3-residue stem region (GCG-UGC) + 4-residue terminal hairpin loop (AUUU)
boxB	GR2 (68 residues)	8-residue basal stem (AUCAGCAU-GUGCUGGU) + single base right bulge (U) + 3-residue stem region (CUA-UAG) + single base left bulge (C) + 2-residue stem region (UG-CA) + 2-residue symmetrical internal loop (C-A) + 4-residue stem region (UGUA-UACA) + 3-residue asymmetrical internal loop (GG-A) + 6-residue stem region (CGAACU-AGUUCG) + 3-residue asymmetrical internal loop (A-AA) + 4-residue stem region (GGUU-AAUC) + 4-residue terminal hairpin (AAGA)

boxB	*Heteroleibleinia fontana* UCFM_HF (69 residues)	8-residue basal stem (AUCAGCAU-GUGCUGGU) + single base right bulge (C) + 3-residue stem region (CUA-UAG) + single base left bulge (C) + 2-residue stem region (UG-CA) + 2-residue symmetrical internal loop (C-C) + 4-residue stem region (UGUA-UACA) + 3-residue asymmetrical internal loop (GA-A) + 5-residue stem region (CGAAC-GUUCG) + 3-residue left bulge (UAG) + 3-residue stem region (GUU-AAC) + single base left bulge (A) + 2-residue stem region (GA-UC) + 4-residue terminal hairpin (GGAA)
	Pseudophormidium sp. ANT.LPE.3 (41 residues)	8-residue basal stem (AUCAGCAA-UUGCUGGU) + single base right bulge (C) + 3-residue stem region (CUA-UAG) + 3-residue asymmetrical internal loop (GG-A) + 5-residue stem region (GAUGU-ACAUC) + 5-residue terminal hairpin (UUGGC)
	Phormidesmis priestleyi ANT.LACV5.1 (50 residues)	8-residue basal stem (AUCAGCAA-UUGCUGGU) + single base right bulge (A) + 3-residue stem region (CUA-UAG) + 3-residue asymmetrical internal loop (GA-G) + 5-residue stem region (GAUGU-ACAUC) + single base right bulge (A) + 4-residue stem region (GAGG-CUUC) + 5-residue terminal hairpin (AAACA)
	Leptolyngbya cf. *fragilis* ANT.L52.1 (50 residues)	7-residue basal stem (AUCAGCA-UGCUGGU) + 3-residue asymmetrical internal loop (A-GC) + 3-residue stem region (CCA-UGG) + 3-residue asymmetrical internal loop (GG-G) + 5-residue stem region (GAUGU-ACAUC) + single base right bulge (A) + 4-residue stem region (GAGC-GUUC) + 5-residue terminal hairpin (AUUAG)
V3	GR2 (77 residues)	2-residue basal stem (GC-GC) + 2-residue symmetrical internal loop (CC-AA) + 13-residue stem region (GAUUAGUAGUGCU-AGCGUUGUUAGUU) + 5-residue asymmetrical internal loop (AAA-AA) + 9-residue stem region (GAUGAUUAU-GUAAUCAUU) + 4-residue symmetrical internal loop (GA-GA) + 2-residue stem region (GU-AC) + 4-residue symmetrical internal loop (AA-AA) + 2-residue stem region (GC-GC) + 4-residue terminal hairpin loop (GCAA)
	Heteroleibleinia fontana UCFM_HF (77 residues)	2-residue basal stem (GC-GC) + 2-residue symmetrical internal loop (CC-AA) + 13-residue stem region (GAUUAGUAGUGCU-GGCGUUGUUAGUU) + single base left bulge (G) + 6-residue stem region (UAGAUA-UGUCUA) + 2-residue symmetrical internal loop (G-A) + 4-residue stem region (UCAU-GUGA) + 4-residue symmetrical internal loop (GA-GA) + 2-residue stem region (GC-GC) + 4-residue symmetrical internal loop (GA-AA) + 2-residue stem region (GU-GC) + 4-residue terminal hairpin loop (GAAA)
	Phormidesmis priestleyi ANT.LACV5.1 (93 residues)	2-residue basal stem (GC-GC) + 5-residue asymmetrical internal loop (CCA-AA) + 3-residue stem region (AUG-CAU) + single base right bulge (G) + 9-residue stem region (AGCUGAGUA-UACUCGGUU) + 6-residue symmetrical internal loop (AAG-AGA) + 3-residue stem region (CGG-CUG) + 2-residue symmetrical internal loop (C-A) + 6-residue stem region (UAGGUA-UAUUUG) + 2-residue symmetrical internal loop (A-C) + 5-residue stem region (GUAAU-GUUAC) + 8-residue symmetrical internal loop (AGAA-GGAC) + 5-residue stem region (GCUAU-AUAGC) + 3-residue terminal hairpin loop (UUA)
	Leptolyngbya cf. *fragilis* ANT.L52.1 (96 residues)	2-residue basal stem (GC-GC) + 5-residue asymmetrical internal loop (CCA-AA) + 4-residue stem region (AUGU-GCAU) + single base right bulge (U) + 9-residue stem region (GCUGAGUA-UGCUCGGU) + 4-residue symmetrical internal loop (GA-GA) + 6-residue stem region (UUAGCC-GGUUGA) + 2-residue symmetrical internal loop (U-U) + 4-residue stem region (UGUA-UAUA) + 2-residue symmetrical internal loop (U-U) + 6-residue stem region (GUAAUG-CGUUAU) + 6-residue symmetrical internal loop (GAA-GGA) + 5-residue stem region (GCUAU-GUAGU) + 6-residue terminal hairpin loop (GUAACA)

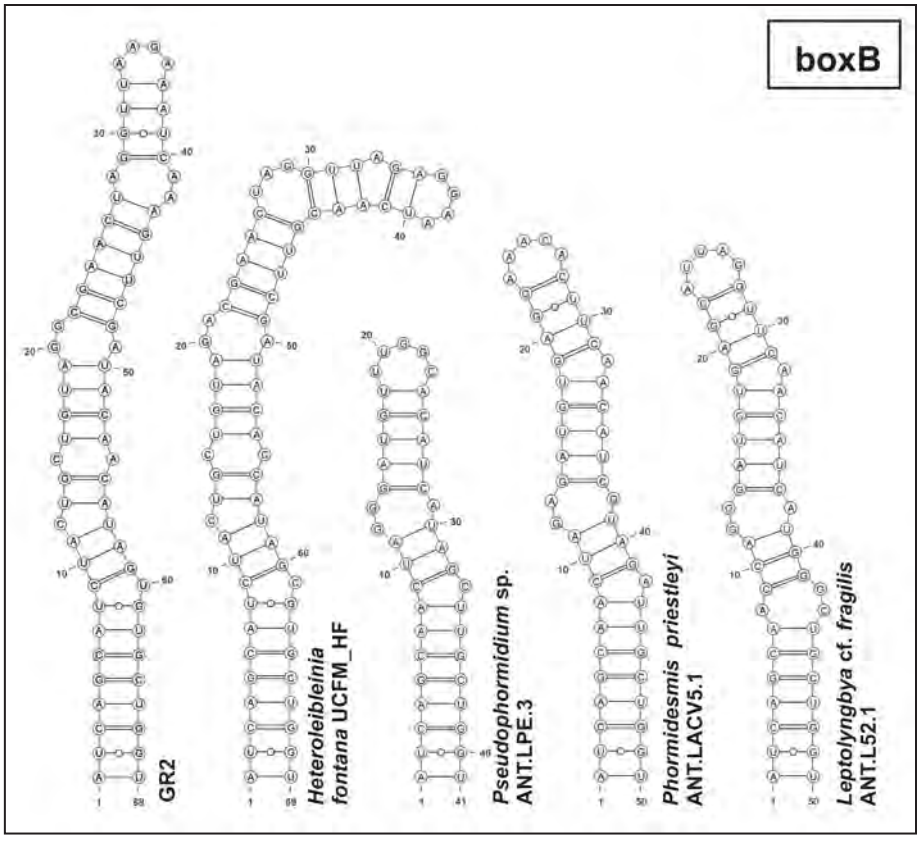

Fig. 7. Hypothetical secondary structures of the 16S-23S ITS region boxB helix for the cyanobacterial strains forming clade A in the 16S-23S ITS phylogenetic reconstruction. In paired regions, A-U pairings are represented with a single line, G-C pairings with a double line, and unconventional pairings with a line interrupted by a circle.

Morphological, cytological and biochemical features

Strain GR2: In culture, strain GR2 was a red-brownish in colour, with some parts of the colony occasionally greenish. Analyses with LM and SEM of this strain highlighted ± curved, densely aggregated filaments (Figs 9 and 12), sometimes twisted to form ropes (Fig. 10). Trichomes were unbranched and constricted at the cell cross walls, without heterocytes (Figs 11-13). The moniliform trichomes were made up by barrel-shaped cells, wider than long (1.2-1.5 μm wide, 0.6-0.9 μm long), and ending with rounded apical cells (Figs 11 and 13). The individual trichomes were surrounded by a sheath (Fig. 9) and frequently the abundant extracellular polysaccharides tightly aggregated the filaments (Fig. 13). Trichome fragmentation occurred without necridia and led to the development of short hormogonia (Fig. 11).

TEM observations evidenced the multilayered structure of the thick sheath (about 300-400 nm thick) (Figs 14-15), cyanophycin granules, and the presence of 5-6 parietal thylakoids arranged in parallel (Figs 14-15). Cell division was symmetrical and perpendicular to the long axis of the trichome (Fig. 15).

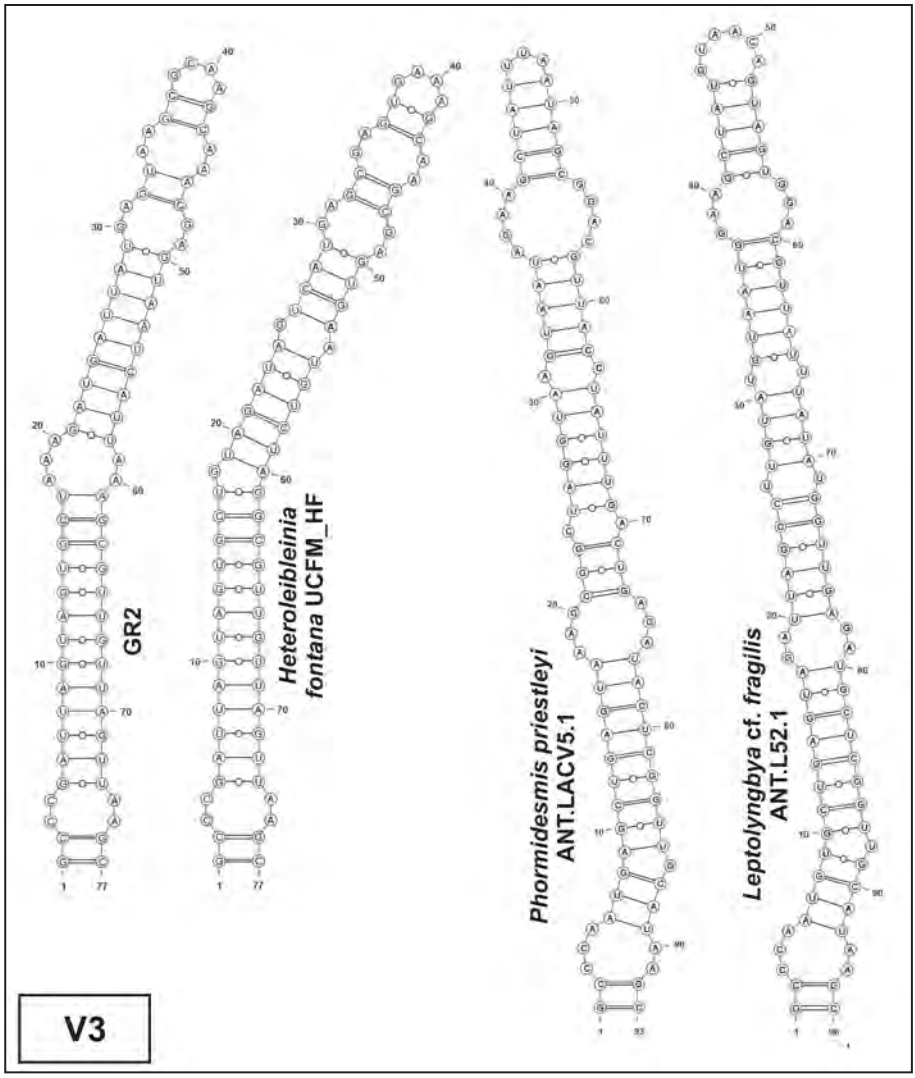

Fig. 8. Hypothetical secondary structures of the 16S-23S ITS region V3 helix for the cyanobacterial strains forming clade A in the 16S-23S ITS phylogenetic reconstruction; the V3 domain of *Pseudophormidium* sp. ANT.LPE.3 was incomplete and therefore the corresponding helix was not inferred. In paired regions, A-U pairings are represented with a single line, G-C pairings with a double line, and unconventional pairings with a line interrupted by a circle.

In the presence of a hard surface, like a calcareous rock, strain GR2 was able to attach to the substrate by one of the filament ends (Figs 16-18).

Spectrophotometric analyses showed the presence of phycoerythrin (41.59 ± 2.33%), C-phycocyanin (38.10 ± 1.99%), and allophycocyanin (20.30 ± 0.92%).

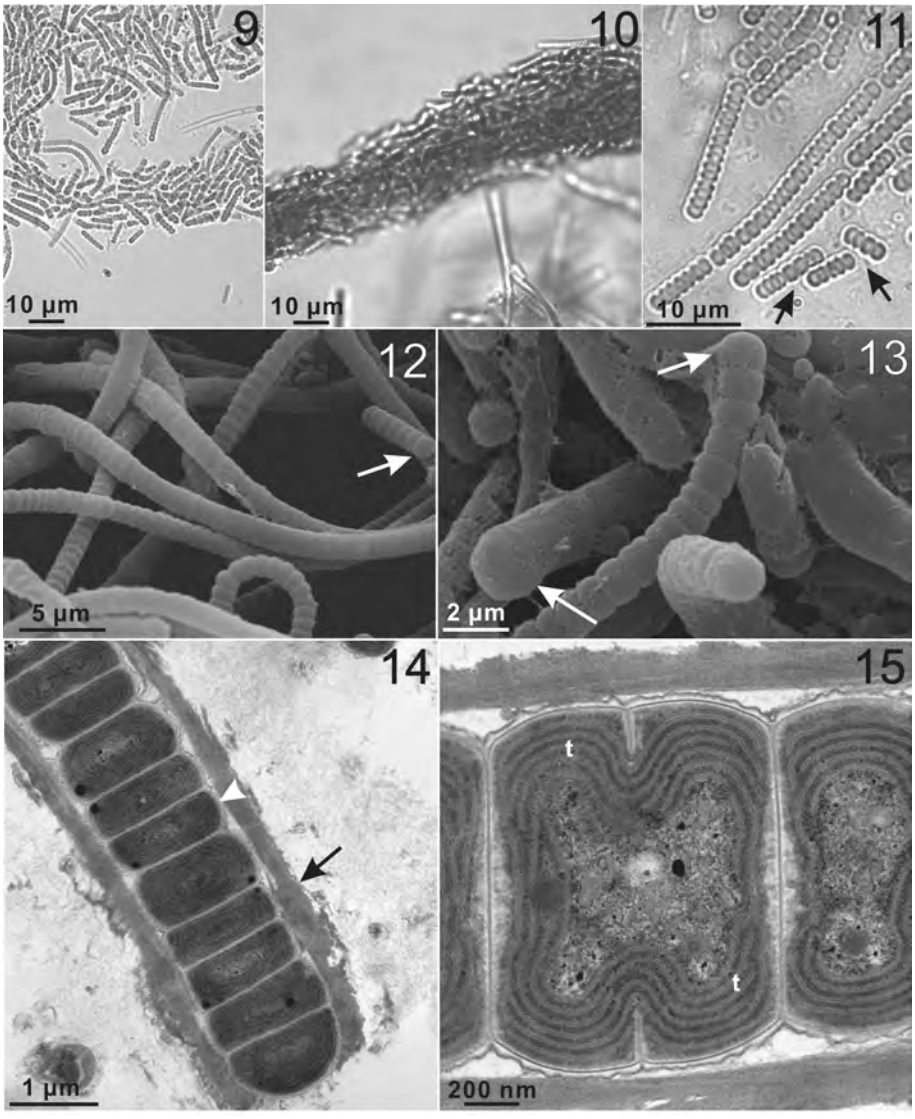

Figs 9-15. Strain GR2. **9-10.** Light microscope images showing unbranched trichomes constricted at the cell cross walls, sometimes forming ropes. **11.** Trichome fragmentation with the development of short hormogonia (arrows). **12-13.** Scanning electron micrographs showing unbranched trichomes constricted at the cell cross walls and ended with rounded apical cells (arrows). **14-15.** Transmission electron microscope images highlighting a trichome with barrel-shaped cells (arrow head), surrounded by a thick sheath (arrow). **15.** Particular of cell in division, characterized by parallel parietal thylakoids (t).

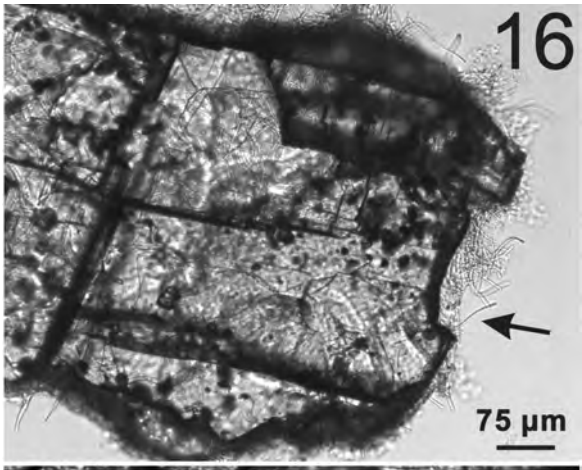

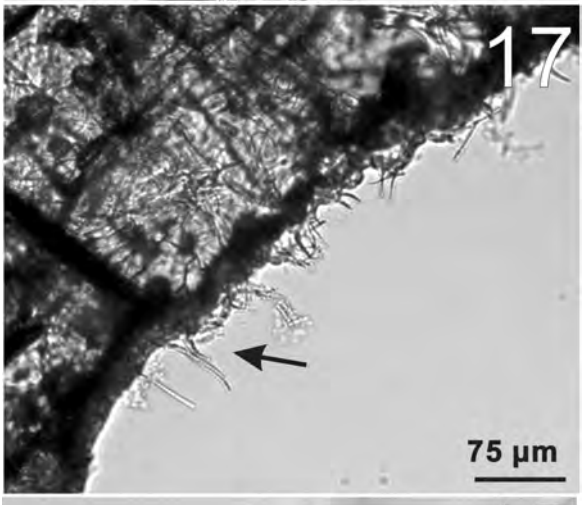

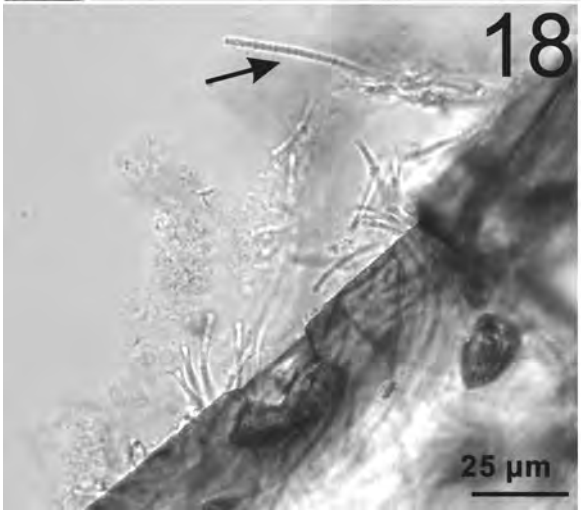

Figs 16-18. Micrographs highlighting strain GR2 capability to attach to the substrate with one of the filament ends. **16.** Overall view of a calcareous stone fragment showing GR2 attachment to the rock surface (arrow). **17-18.** Details at different magnifications of attached GR2 filaments (arrows).

Strain GR4: Strain GR4 cultures were red-brown in colour. Using the LM this non-heterocytous strain exhibited flexuous curved filaments (Fig. 19), surrounded by a colourless sheath and with false branching (Figs 20-21). Trichomes, slightly constricted at the cross wall, consisted of cells from isodiametric to longer than wide (1.7-4.4 µm long, 1.2-1.8 µm wide) (Fig. 21); apical cells were rounded (Fig. 20). Also in strain GR4 the cell division was symmetrical and perpendicular to the long axis of the filament, but occasionally it was oblique (Fig. 20), forming branches. Observed by SEM, the sheaths, individually surrounding the filaments, were sometimes anastomosed and fused (Figs 22-23). Observations with TEM showed the trichomes to be slightly constricted at the cell cross wall and the presence of multilayered sheaths, thicker than 500 nm (Figs 24-26). Moreover, the isodiametric

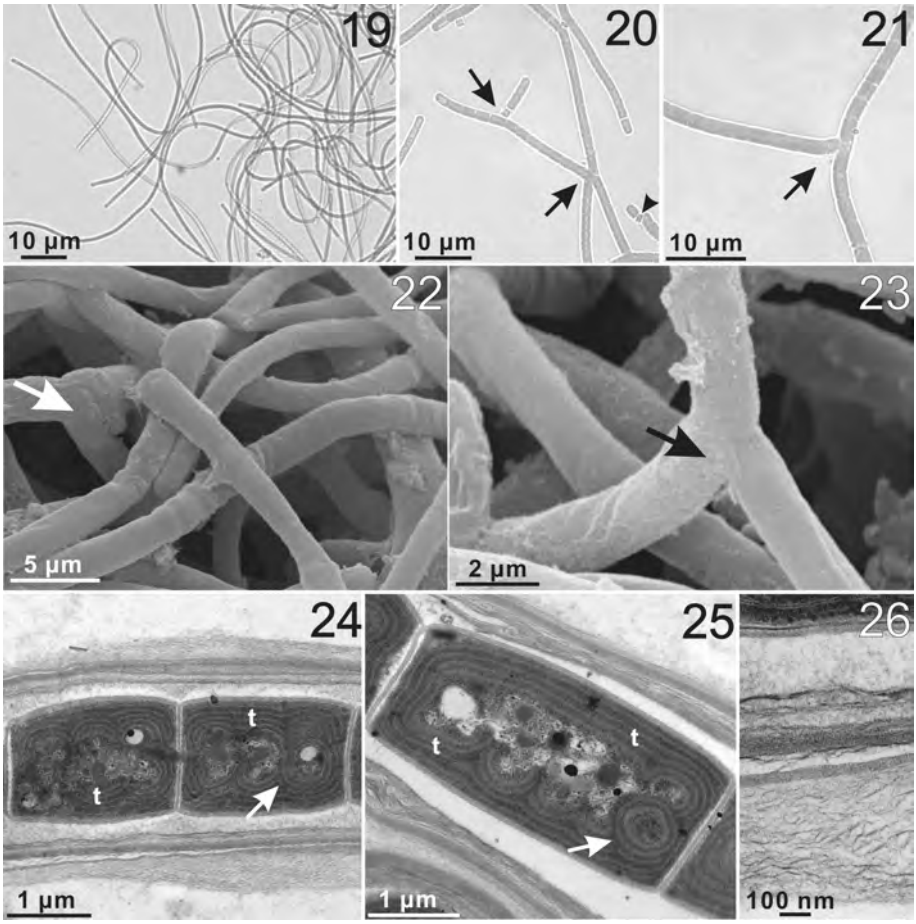

Figs 19-26. Strain GR4. **19-21.** Light micrographs showing flexuous trichomes, characterized by branching (arrows). Note in **20** the oblique cell division, giving rise to branching (arrow head). **22-23.** Scanning electron microscope images of trichomes surrounded by a conspicuous sheath. Note the presence of a branch (arrow). **24-25.** Transmission electron microscope images showing lightly barrel-shaped cells, characterized by parietal thylakoids (t), sometimes arranged in circular way (arrow). **26.** Particular of a multilayered sheath, surrounding the filaments.

cells showed 5 parietal thylakoids, which in some areas appeared to be organized in a circular arrangement (Figs 24-25).

Water-soluble pigments were phycoerythrin (53.52 ± 1.59%), C-phycocyanin (40.86 ± 1.57%) and allophycocyanin (5.61 ± 0.74%).

Strain GR13: Strain GR13 cultures were red-brown in colour, darker than those of strain GR4. With LM strain GR13 appeared non-heterocytous and formed by very long, flexuous, and curved trichomes (Fig. 27), surrounded by a colourless sheath, and characterized by the presence of different types of false branching (Figs 28-29); the first type of branching occurred for trichome fragmentation and lateral protrusion through the sheath (Fig. 28), the second one was a *Scytonema*-type false branching (Fig. 29). Each trichome was composed by longer than wide cells, 3.2-4.2 µm in length and 1.2-1.4 µm in width, and showed constrictions at the cell

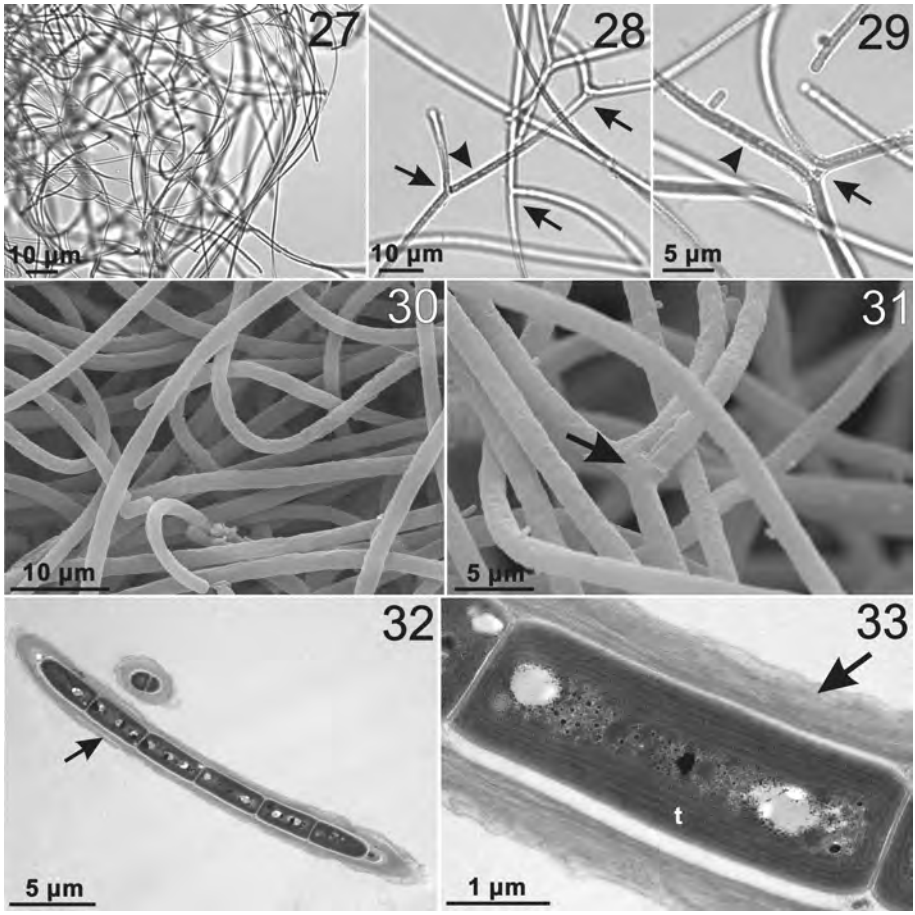

Figs 27-33. Strain GR13. **27-29.** Light microscope images showing curved trichomes, branched (arrows) and surrounded by a colorless sheath (arrow head). **30-31.** Scanning electron micrographs of trichomes surrounded by a conspicuous sheath. Note in (31) the presence of a three-forked branching (arrow). **32-33.** Transmission electron microscope pictures of ultrastructure of trichomes. Note in the cells the parietal arrangement of the parallel thylakoid (t) and the presence of the multilayered sheath (arrow).

cross wall (Fig. 29); apical cells were rounded (Fig. 29). The cell division was symmetrical and perpendicular to the long axis of the filament; however occasionally it was oblique, giving rise to branches (Fig. 28).

SEM observations highlighted conspicuous sheaths surrounding each filaments, sometimes anastomosed (Fig. 30), and the presence of branching. Occasionally, the *Scytonema*-type branching was characterized by a branch shorter than the other, appearing three-forked like a trident (Fig. 31). TEM analyses showed that the sheath was multilayered and 4-6 thylakoids, arranged in parallel at the periphery of the cells (Figs 32-33).

Strain GR13 exhibited a dominance of phycoerythrin (64.68 ± 6.82%) over C-phycocyanin (30.89 ± 8.79%) and allophycocyanin (4.44 ± 1.99%).

Published data on the other strains included in clade A

In the case of clade A, morphological data and LM pictures were available for the strains *Leptolyngbya* sp. CYN64 and *Leptolyngbya* sp. CYN68 (Martineau *et al.*, 2013). Strain CYN64 is a blue-green, non-heterocytous cyanobacterium, with cells longer than wide (1.2-2.1 μm wide, 1.6-4.1 μm long), and rounded apical cells. Martineau *et al.* (2013) initially attributed this strain to the genus *Pseudanabaena* Lauterborn, since they did not observe a sheath surrounding the trichomes; however the phylogenetic analyses carried out by the same authors showed the relatedness of strain CYN64 with other Antarctic strains ascribed to the genus *Leptolyngbya*. Moreover, by observing the image of CYN64 LM (Fig. 1A in Martineau *et al.*, 2013) we clearly detected a sheath surrounding the trichomes. Strain CYN68 is a blue-green, non-heterocytous cyanobacterium, forming a dense tangled mat; it was morphologically attributed to the genus *Leptolyngbya* by Martineau *et al.* (2013), but it did not match with any known cyanobacterial taxa based on the molecular analyses carried out by these authors. Cells of the trichomes of strain CYN68 are longer than wide (1.3-1.9 μm wide, 1.1-4.3 μm long) and the apical cells are tapered; a sheath surrounding CYN68 trichomes is clearly visible in the LM picture of this strain (Fig. 1E in Martineau *et al.*, 2013). Strains CYN64 and CYN68, both sampled from benthic mats in shallow melt-water ponds in Antarctica, clustered with high statistical support in the 16S rRNA phylogenetic tree reported by Martineau *et al.* (2013). Morphological data were not available for the other strains included in clade A; the available ecological and geographical data are reported in Table 1.

Published data on the other strains included in clade B

For clade B, morphological data and/or pictures were available for more strains. A complete description, including several pictures, is available for *H. fontana* UCFM_HF, an epilithic cyanobacterium isolated from the Kaituna river, Banks Peninsula, New Zealand (Merican, 2013). It is a blue-green, filamentous, non-heterocytous cyanobacterium, ascribed to the genus *Heteroleibleinia* for its ability to attach to the substrate with one end of the filaments. In strain UCFM_HF, the heteropolar trichomes are ensheathed, constricted at the cross-walls, and composed of barrel-shaped cells, isodiametric or shorter than wide (2.4-3.0 μm wide, 0.8-1.6 μm long); the apical cells are obtusely rounded (Merican, 2013). Another strain for which a complete description was available is *Plectonema* sp. F3 (Wilmotte, 1991); this is a coastal marine, blue-green, filamentous, non-heterocytous cyanobacterium, with trichomes constricted at the cross-walls and surrounded by a

thin colourless sheath. Trichomes are composed of isodiametric to shorter than wide cells (1-2 μm wide, 0.8-1.6 μm long) and the apical cells are rounded or conical. False branching was rarely observed in strain F3 (Wilmotte, 1991). Some ecological and morphological data are available also for strain FBP256 (De la Torre *et al.*, 2003), isolated from a cryptoendolithic community in Antarctica and cultivated in laboratory, showing optimal growth at 4°C and 15°C and preferring oligotrophic media. De la Torre *et al.* (2003) described it as a coccoid cyanobacterium, with 5 μm wide cells, although their phylogenetic reconstruction related strain FBP256 with filamentous cyanobacteria attributed to the genera *Phormidium* and *Plectonema* (Fig. 2 in De la Torre *et al.*, 2003). Indeed, the LM picture of strain FBP256 (Fig. 6 in De la Torre *et al.*, 2003) shows short moniliform trichomes and a large number of hormogonia.

For *Phormidesmis priestleyi* ANT.LACV5.1 and *Leptolyngbya* cf. *fragilis* ANT.L52.1, LM pictures are available for the BCCM/ULC cyanobacterial collection (http://bccm.belspo.be/catalogues/ulc-catalogue-search). Strain ANT.LACV5.1 is deposited at BCCM/ULC under the accession number ULC035, where it is kept at a temperature of 12°C; it is a blue green filamentous cyanobacterium, characterized by long moniliform trichomes, constricted at the cross-walls, composed of isodiametric cells (0.8-1.5 μm wide, 0.9-2.9 μm long) and with rounded or pointed apical cells; each trichome is surrounded by a thin colourless sheath. Strain ANT. L52.1 is deposited in BCCM/ULC under the accession number ULC004, where it is maintained at a temperature of 18°C; it is an olive-green filamentous cyanobacterium, lacking heterocytes, and made up of moniliform trichomes, about 2 μm wide, distinctly constricted at the cross-walls and surrounded by a colourless sheath. Inside trichomes the cells are isodiametric; the apical cells are rounded and sometimes enlarged. There are no further morphological data for other cyanobacterial strains forming clade B; data regarding the habitat and the collection sites data are reported in Table 2.

DISCUSSION

Based on 16S rRNA and 16S-23S ITS phylogenetic reconstruction, our Giant Cave cyanobacteria belong to two distinct and well-supported lineages: strains GR4 and GR13 are in clade A, while strain GR2 is placed in clade B. The high statistical support for these two clades, as well as the 16S rRNA similarities inside the two groups, suggest that they represent two lineages distinct from the existing genera of the family Leptolyngbyaceae with sequences to date. In particular, both clades A and B 16S rRNA percent identities are above the threshold (95%) proposed by Stackebrandt & Goebel (1994) to assign two prokaryotes to the same genus. Although fewer strains were included, these two newly detected lineages were also indirectly found in previous investigations, most of which were ecological surveys of particular environments. A group corresponding to clade A is shown by Arp *et al.* (2010) and Taton *et al.* (2006a); highly supported clades equivalent to clade B are reported in De la Torre *et al.* (2003), Lamprinou *et al.* (2012b), Taton *et al.* (2006b), Olsson-Francis *et al.* (2010), and Taton *et al.* (2011).

Over the last few years, the analysis of 16S-23S ITS secondary structures, associated with the 16S rRNA phylogenies, has become a useful tool for detecting cyanobacterial taxa and for identifying new genera and species (e.g., Johansen *et al.*,

2011; Perkerson *et al.*, 2011; Zammit *et al.*, 2012; Osorio-Santos *et al.*, 2014; Dvořák *et al.*, 2015; Vaz *et al.*, 2015; Miscoe *et al.*, 2016; Sciuto & Moro, 2016). However, in this study the interpretation of the 16S-23S ITS secondary structure results was not straightforward. In clade A, the D1-D1' helix, usually one of the most conserved ITS region domains (Iteman *et al.*, 2000; Perkerson *et al.*, 2011; Osorio-Santos *et al.*, 2014; Vaz *et al.*, 2015; Sciuto & Moro, 2016) and recently proposed as a tool to distinguish between different genera (Sciuto & Moro, 2016), is highly variable, except for strains GR4 and GR13 which had similar D1-D1' secondary structures. Conversely, the boxB helix and, in particular, the V3 helix, usually considered more variable (Iteman *et al.*, 2000; Perkerson *et al.*, 2011; Osorio-Santos *et al.*, 2014; Vaz *et al.*, 2015; Sciuto & Moro, 2016), were more congruent and thus indicated that clade A strains belong to the same genus. It is worth underlining that other studies have shown a high D1-D1' helix variability among species belonging to the same cyanobacterial genus (e.g., Dvořák *et al.*, 2015) or at least in one or a few species belonging to a given genus (e.g., Johansen *et al.*, 2011; Osorio-Santos *et al.*, 2014).

For clade B, the interpretation of the 16S-23S ITS secondary structure data was complicated as well. In fact, the inferred D1-D1' helices are compatible with the hypothesis that clade B strains belong to the same genus, thus supporting the 16S rRNA and ITS region phylogenetic analyses. This is partially suggested also by the boxB helix, which recently has been suggested for drawing distinctions both at the genus and species levels (Sciuto & Moro, 2016). However, the boxB helix, and, in particular, the V3 helix results indicate separation among the clade B strains, with strain GR2 more related to *H. fontana* UCFM_HF and showing several differences with respect to the other cyanobacteria included in this phylogenetic lineage.

With regard to ecology and geography, some general trends can be seen for both clade A and clade B strains. The cyanobacteria clustering in these two phylogenetic lineages were mainly sampled from aerophytic or subaerophytic habitats, and even when found in aquatic habitats they were generally isolated from benthic mats; most of them are epilithic or endolithic (Tables 1 and 2; e.g., Smith *et al.*, 2000; De la Torre *et al.*, 2003; Olsson-Francis *et al.*, 2010; Perkerson *et al.*, 2011; Chong *et al.*, 2012; Merican, 2015; Arp *et al.* 2016; Strunecky *et al.*, unpublished) like *Lampenflora* strains GR2, GR4 and GR13 that were isolated from calcareous rocks.

Clade B cyanobacteria also seem to have a wide salinity tolerance; there are cyanobacteria reported from hyposaline lakes (e.g., Taton *et al.* 2006a) or classified as "non-halophilic" (Smith *et al.*, 2000), cyanobacteria found in transitional environments (Taton *et al.*, 2003; Chong *et al.*, 2012), and coastal marine cyanobacteria, which undergo periods of immersion and emersion according to the tidal cycles (Wilmotte, 1991; Olsson-Francis *et al.*, 2010). Among clade A strains, only the cyanobacterial clone Fr094 is reported from a brackish lake (Taton *et al.*, 2003), while the others were detected in freshwater, soil, or subaerophytic habitats (Table 1).

Both clade A and clade B cyanobacteria seem to tolerate low temperatures; this is underlined by the fact that most of the strains were reported from Antarctica and from mountain environments (Fig. 1, Tables 1 and 2) and, in the case of clade A, there were also two Arctic cyanobacteria. A lineage very probably corresponding to clade A was previously reported by Chrismas *et al.* (2012) in a study concerning the relationship between polar and alpine cyanobacteria; this clade (clade J of Fig. 3 in Chrismas *et al.*, 2012) is one of the lineages predicted to have a most recent cold-tolerant common ancestor.

Another interesting feature is the tolerance to UV radiation by the clade A cyanobacterium *Leptolyngbya* sp. OU_6 shown by Olsson-Francis *et al.* (2010); in the Giant Cave the *Lampenflora* is routinely exposed to UV lamps, which are used during the night with the aim of preventing its growth.

Returning to the investigated Giant Cave cyanobacteria, the data obtained in this study as a whole highlight the relatedness between strains GR4 and GR13 and their belonging to a new genus represented by clade A. Interestingly, a previous study by Martineau *et al.* (2013) suggested that strain CYN68, here included in clade A, could belong to an undescribed cyanobacterial taxon and Arp *et al.* (2010) considered strain WB1.10, here likewise part of clade A, as belonging to an unidentified lineage. The genus represented by clade A is a cryptogenus, i.e. ‘‘a genus that can be only detected based on molecular and phylogenetic analyses, not showing distinctive morphological and/or ecological features” (Komárek *et al.*, 2014). Besides the above discussed evidence based on the 16S rRNA gene, the analysis of the ITS region secondary structures also supports the hypothesis that clade A represents a new genus. This is evident by comparing the ITS region secondary structures of clade A with those of “*Leptolyngbya frigida*” clade, the lineage that is more related to clade A in both phylogenetic analyses. Although the D1-D1’ and boxB helices of clade A showed a certain variability, they were comparable in the basal part; the D1-D1’ and boxB helices of “*L. frigida*” clade are different from those of clade A even in the basal portion. The V3 helices of clade A strains were, instead, very congruent; the V3 helix obtained for “*L. frigida*” clade is completely different from those of clade A and this is further highlighted by the presence of an asymmetrical internal loop and of a left bulge near the base that make the “*L. frigida*” V3 helix curve to the right. We compared the ITS region secondary structures of clade A also with those published for the genus *Leptolyngbya* (Sciuto & Moro, 2016), the type genus of the family Leptolyngbyaceae. Indeed, the 51-residue structures predicted for the D1-D1’ helix of the genus *Leptolyngbya* (Figs 6C and 6D in Sciuto & Moro (2016)) are very different from those found for clade A. The same can be said for the boxB helices, 33 residues long (Figs 10C and 10D in Sciuto & Moro (2016)), and for the very short V3 helix (Fig. 9C in Sciuto & Moro (2016)) of the genus *Leptolyngbya*.

The position of strains GR4 and GR13 in the phylogenetic reconstructions and the percentage identity between their 16S rRNA sequences suggest that they belong to different species. In particular, strains GR4 and GR13 shared a 16S rRNA percent identity of 98.65% based on an alignment of 1119 positions and the interspecific ranges of 16S rRNA percent identities, calculated on the same alignment, were 98.47-99.73% for the genus *Leptolyngbya*, 96.95-99.10% for the genus *Oculatella*, and 99.46% for the genus *Thermoleptolyngbya* (Fig. S5, see doi/10.7872/crya/v38.iss4.2017.Suppl.Mat.).

The differences detected in the 16S-23S ITS secondary structures of strains GR4 and GR13 also lead us to suppose they belong to separate species. In particular, the central part of D1-D1’ helix and the second part of the boxB helix were very variable between the two strains; moreover, in the D1-D1’ helix a CBC and two hCBCs were found in the conserved terminal portion and in the boxB helix two hCBCs were present in the first conserved part. The hypothetical structures obtained for the V3 helix of strains GR4 and GR13 were very congruent, with two structural differences only in the terminal part; however one CBC and four hCBCs were observed in the conserved portion of V3 helix. In eukaryotes, if two organisms differ for even a CBC in given conserved regions of their ITS2 secondary structures, the two organisms belong to different species with a probability of 93% (Müller *et al.*,

2007; Coleman, 2009; Wolf *et al.*, 2013). Obviously, here we are dealing with prokaryotes and this rule cannot be applied, but it is worth underlining that strains GR4 and GR13 have accumulated enough evolutionary distance to generate CBCs in the conserved portions of their ITS region helices.

A morphological feature allows the distinction between strains GR4 and GR13 kept under the same culture conditions and observed at the same time of their life cycle. Several cells of strain GR4 always had thylakoids organized concentrically, while strain GR13 cells did not. To our knowledge this particular thylakoid formation has so far been observed only in *Plectolyngbya hodgsonii* Taton *et al.* (Taton *et al.*, 2011). We consider the circular arrangement of thylakoids to be a diagnostic character that further supports the separation of strains GR4 and GR13 into two different species of the new genus *Timaviella*.

Regarding strain GR2, based on 16S rRNA available data, it is most closely related to three uncharacterized cyanobacteria (clone BGC-Fr054, isolate OUT 00162, strain QSSC8cya), *P. priestleyi* ANT.LPR2.6, and *H. fontana* UCFM_HF. The 16S rRNA percent identities calculated on the alignment used for the phylogenetic analyses suggest a stronger relationship both between strain GR2 and *P. priestleyi* ANT.LPR2.6 and between *H. fontana* UCFM_HF and *P. priestleyi* ANT.LPR2.6 than between strain GR2 and *H. fontana* UCFM_HF. However, we cannot exclude the possibility that the calculated 16S rRNA identity values are due to the short alignment used; indeed, the longer 16S rRNA alignment between GR2 and *P. priestleyi* ANT.LPR2.6 gave a slightly lower percentage identity, because of the higher number of nucleotide substitutions in the first portion of the 16S rRNA gene, which was not available for *H. fontana* UCFM_HF (Fig. S6, see doi/10.7872/crya/v38.iss4.2017.Suppl.Mat.). Phylogenetic reconstruction and secondary structure analysis of the 16S-23S ITS locus suggest that strain GR2 is more related to *H. fontana* UCFM_HF than to the other cyanobacteria included in clade B; unfortunately, the 16S-23S ITS region sequence was not available for *P. priestleyi* ANT.LPR2.6. Based on the available molecular data, we can conclude that strain GR2, *H. fontana* UCFM_HF, and *P. priestleyi* ANT.LPR2.6 are strongly allied and that they very probably belong to the same genus.

In the 16S rRNA tree, two cyanobacteria belonging to clade B were named *Plectonema* sp. F3 and *Pseudanabaena minima* SABC031701. These two strains had a 16S rRNA sequence identity of 100% (Fig. S2, see doi/10.7872/crya/v38.iss4.2017.Suppl.Mat.) and thus, very probably, they belong to the same taxonomic unit. We have no morphological data for *P. minima* SABC031701, but information is available for *Plectonema* sp. F3 and they are comparable with the morphological and ecological data that we were able to retrieve for other clade B strains. Komárek & Anagnostidis (2005) questioned the real existence of the genus *Plectonema* Thuret ex Gomont, the main diacritical feature of which is the obligatory presence of tolypotrichoid or scytonematoid false branching, with trichomes usually 8-25 µm wide. This taxon underwent several revisions during years, with the re-attribution of many species to other genera, in particular to the genera *Leptolyngbya* and *Pseudophormidium* (Komárek & Anagnostidis, 2005; Komárek *et al.*, 2014). For these reasons, we exclude the possibility that strain F3 belongs to the genus *Plectonema* and that clade B can coincide with this taxon.

In both the performed phylogenetic analyses, besides the above reported genera *Heteroleibleinia* and *Phormidesmis*, some clade B strains were tentatively attributed also to *Leptolyngbya* and *Pseudophormidium*; all these different genera show overlapping morphological features (Table S1, see doi/10.7872/crya/v38.iss4.2017.Suppl.Mat.). The genus *Pseudophormidium* (Forti) Anagnostidis &

Komárek is always richly pseudobranched (Komárek & Anagnostidis, 2005) and it was recently attributed to the family Microcoleaceae (Komárek *et al.*, 2014). This genus, as originally described, is very probably composed of more than one taxon and it needs a revision (Komárek *et al.*, 2014). For these reasons, we exclude that clade B can coincide with the genus *Pseudophormidium* as currently intended.

Cyanobacteria regarded as genuine representatives of the genera *Leptolyngbya* Anagnostidis & Komárek (e.g., Moro *et al.*, 2010; Johansen *et al.*, 2011; Osorio-Santos *et al.*, 2014; Sciuto & Moro, 2016) and *Phormidesmis* Turicchia *et al.* (Komárek *et al.*, 2009; Turicchia *et al.*, 2009) were included in the phylogenetic analyses and formed two different lineages that, in both the phylogenetic reconstructions, were placed far from clade B. Therefore, clade B cannot match either of these taxa as well.

The remaining cyanobacterium of clade B that was taxonomically determined is *H. fontana* UCFM_HF, to which strain GR2 is phylogenetically strongly related. The genus *Heteroleibleinia* (Geitler) Hoffmann originally belonged to the family Pseudanabaenaceae, subfamily Heteroleibleinioideae (Komárek & Anagnostidis, 2005), but it was recently transferred to the family Heteroleibleinaceae, together with the genus *Tapinothrix* Sauvageau (Komárek *et al.*, 2014). According to Komárek *et al.* (2014), the family Heteroleibleinaceae is strongly allied with the family Leptolyngbyaceae, from which it can be distinguished only for the attachment to the substrate by one of the filament ends. However, the authors state that "more evidence is needed to establish the family as independent from Leptolyngbyaceae" (Komárek *et al.*, 2014).

As other features, the heteropolar attachment to the substrate is usually lost in laboratory culture conditions (Merican, 2013; Komárek *et al.*, 2014) and we did not observe the habit of strain GR2 in the environment where it was sampled. It is also worth underlining that, for some *Heteroleibleinia* species like *H. epiphytica* (Wille) Komárek in Anagnostidis, strains with attached heteropolar trichomes and strains characterized by isopolar trichomes with both ends free have been described (Komárek & Anagnostidis, 2005). However, we carried out a laboratory experiment that highlighted the ability of strain GR2 to attach to hard surfaces with one end of the filaments, thus further suggesting its belonging to the genus *Heteroleibleinia.* Of the species listed within this genus, based on the morphological, biochemical, and geographical data, strain GR2 probably represents the species *H. purpurascens* (Hansgirg) Anagnostidis & Komárek. Besides the cell sizes, which are 1.5-2 μm wide and 0.5 times as long as wide to isodiametric, other features of *H. purpurascens* description match the habit of strain GR2. In particular, the densely aggregated filaments, most of which very short (30-60 μm) and each surrounded by a colourless sheath, macroscopically form a thin membranaceous, purple to brownish violet thallus. With LM, the trichome colour of *H. purpurascens* can vary from purple, to violet, to blue-green or olive-brownish, as in the case of strain GR2. Also, the sampling site of strain GR2 fits with the habitat and the geographical distribution of *H. purpurascens*: this is a freshwater species, able to live in subaerophytic habitats, that was reported from central-European mountains, including the Austrian Alps (Komárek & Anagnostidis, 2005), from Northern American mountain environments (Johansen *et al.*, 2007), and from New Zealand streams (Bray *et al.*, 2008).

The 16S rRNA phylogenetic reconstruction included also the sequence of *Tapinothrix clintonii* GSE-PSE06-07G (HQ132936), the only member of this genus for which molecular data are available so far. The genus *Tapinothrix* was placed in the family Heteroleibleiniaceae by Komárek *et al.* (2014) with *Heteroleibleinia*, based on the heteropolar attachment of the filaments to the substrate. Bohunická

et al. (2011) showed that *Tapinothrix clintonii* Bohunická & Johansen was closely related to the genus *Leptolyngbya*, at that time still included in the family Pseudanabaenaceae. Our molecular results confirm this relationship and show the alliance of *T. clintonii* with the genus *Plectolyngbya* as well. We did not find a strong relationship between *T. clintonii* and the two species of *Heteroleibleinia* (*H. fontana* and *H. purpurascens*) considered in our analyses. Therefore, the present data, as well as the findings by Bohunická *et al.* (2011), do not support the existence of the family Heteroleibleinaceae; however, further investigations, including more strains and species of the genera *Tapinothrix* and *Heteroleibleinia*, are required in this regard.

CONCLUSION

This study represents the first survey on the *Lampenflora* of the Giant Cave based on a polyphasic approach. The data collected suggest that clade A corresponds to a new genus within the family Leptolyngbyaceae and that the Giant Cave strains GR4 and GR13 represent two distinct species of this new taxon. Therefore, we propose the taxonomic treatment reported below.

The obtained results also suggest that clade B represents a distinct lineage of the family Leptolyngbyaceae; however we could directly describe only a strain inside this group, while for the other cyanobacteria included in clade B we could only analyse the available published data. The fact that many clade B strains have been attributed to different taxa (*Heteroleibleinia*, *Leptolyngbya*, *Phormidesmis*, *Plectonema*, and *Pseudophormidium*) by experienced authors underlines, once again, the difficulty of identifying and distinguishing certain cyanobacterial taxa, characterized by few diagnostic characters and/or with overlapping morphologies. We will not propose a new genus corresponding to clade B nor state that the entire clade B represents the genus *Heteroleibleinia* based only on the present study; in this regard further investigations are necessary. Nevertheless, considering the above reported data, we attribute strain GR2 to *Heteroleibleinia purpurascens* (Hansgirg) Anagnostidis & Komárek; this strain is the second member of the controversial genus *Heteroleibleinia* for which molecular data are available (the other is *H. fontana* UCFM_HF) and the first *Heteroleibleinia* strain to be available in a public culture collection.

Taxonomic treatment

Timaviella Sciuto & Moro **gen. nov.**

Phylum: Cyanobacteria
Order: Synechococcales
Family: Leptolyngbyaceae
Description: Long flexuous and curved filaments, red-brown in colour. Trichomes, often false branched, slightly constricted at the cross wall, surrounded by a multilayered colorless sheath. Cells from isodiametric to longer than wide, 1.1-4.4 μm long and 1.2-2.1 μm wide, with parietal thylakoids. Apical cells rounded or tapered. Reproduction by fragmentation of trichomes in short hormogonia, without necridic cells. Distributed in mountain and polar environments; occurring in freshwater and subaerophytic habitats, such as wet soils and wet rock surfaces.

Diagnosis: circumscribed by molecular and phylogenetic analyses based on the 16S rRNA gene and the 16S-23S ITS region. The 16S-23S ITS region with distinctive boxB and V3 helices.
Etymology: the generic name "*Timaviella*" (fem. noun.) was derived from the mysterious river Timavo, which is part of the Reka-Timavo hydrogeological complex, in turn included in the Italian-Slovenian Karst system (Civita *et al.*, 1995; Cucchi *et al.*, 2015). This generic name was chosen because the Timavo river is involved in the formation of Karst caves, but also for the parallelism between the hidden nature both of this river and of the genus *Timaviella*.
Type species: Timaviella circinata Sciuto & Moro.

Timaviella circinata Sciuto & Moro **sp. nov.** **Figs 19-26**

Description: Filaments long, flexuous and curved, red-brownish, characterized by the presence of false branching. Sheaths colourless, multilayered, thick. Trichomes, without heterocytes, slightly constricted at the cross wall. Cells from isodiametric to longer than wide (1.7-4.4 μm long, 1.2-1.8 μm wide), with 5 parietal thylakoids, frequently organized in a circular arrangement. Apical cells rounded. Cell division symmetrical and perpendicular to the long axis of the filament, but occasionally oblique, forming branches. Water-soluble pigments: phycoerythrin, C-phycocyanin, and allophycocyanin.
Diagnosis: detected by molecular and phylogenetic analyses based on the 16S rRNA gene and 16S-23S ITS region. 16S-23S ITS region with distinctive boxB and V3 helices. Distinguished from the only other species so far described under the genus *Timaviella* for the particular arrangement of the thylakoids that frequently appear concentric.
Type locality: The Giant Cave ("Grotta Gigante" in Italian) located in the alpine area (Oriental Alps), in the municipality of Sgonico, Trieste, North-Eastern Italy (45°42'35.62''N; 13°45'52.33''E).
Etymology: the specific epithet *circinata* (fem. adj.) refers to the arrangement of thylakoids, which are frequently concentric.
Holotype: resin-embedded sample of strain GR4 deposited at PAD (A000629).
Living cultures: a living culture of strain GR4 is available at the BCCM/ULC Cyanobacteria collection (Centre for Protein Engineering, University of Liège, Belgium), under code ULC401.
DNA sequences available: LT634149 (16S rRNA gene), LT634152 (16S-23S ITS region).

Timaviella karstica Sciuto & Moro **sp. nov.** **Figs 27-33**

Description: Long flexuous and curved trichomes, non heterocytous, red-brownish, surrounded by a multilayered colourless sheath. False branched trichome, occasionally appearing as three-forked. Filaments slightly constricted at the cross wall. Cells longer than wide (3.2-4.2 μm long, 1.2-1.4 μm wide), with 4-6 peripherally arranged thylakoids. Apical cells rounded. Cell division symmetrical and perpendicular to the long axis of the filament, but occasionally oblique, forming branches. Pigments phycoerythrin-rich.
Diagnosis: detected by molecular and phylogenetic analyses based on the 16S rRNA gene and 16S-23S ITS region. 16S-23S ITS region with distinctive boxB and V3 helices.
Type locality: The Giant Cave ("Grotta Gigante" in Italian) located in the alpine area (Oriental Alps), in the municipality of Sgonico, Trieste, North-Eastern Italy (45°42'35.62''N; 13°45'52.33''E).

Etymology: the specific epithet *karstica* (fem. adj.) means of Karst.
Holotype: resin-embedded sample of strain GR13 deposited at PAD (A000630).
Living cultures: a living culture of strain GR13 is available at the BCCM/ULC Cyanobacteria collection (Centre for Protein Engineering, University of Liège, Belgium), under code ULC402.
DNA sequences available: LT634150 (16S rRNA gene), LT634153 (16S-23S ITS region).

Acknowledgements. We thank Prof. Christine A. Maggs for her support and for helping with manuscript revision.

REFERENCES

ALTSCHUL S.F., GISH W., MILLER W., MYERS E.W. & LIPMAN D.J., 1990 — Basic local alignment search tool. *Journal of molecular biology* 215: 403-410.

ARP G., BISSETT A., BRINKMANN N., COUSIN S., DE BEER D., FRIEDL T., MOHR K.I., NEU T.R., REIMER A., SHIRAISHI F., STACKEBRANDT E. & ZIPPEL B., 2010 — Tufa-forming biofilms of German karstwater streams: microorganisms, exopolymers, hydrochemistry and calcification. *In*: Pedley H.M. & Rogerson M. (Eds), *Tufas and Speleothems: Unravelling the Microbial and Physical Controls*. London, Geological Society, Special Publications, pp. 83-118.

ASENCIO A., ABOAL M. & HOFFMANN L., 1996 — A new cave-inhabiting blue-green alga: *Symphyonema cavernicolum* sp. nova (Mastigocladaceae, Stigonematales). *Algological studies* 83: 73-82.

BENNET A. & BOGORAD L., 1973 — Complementary chromatic adaptation in a filamentous blue-green alga. *Journal of cell biology* 58: 419-435.

BOHUNICKÁ M., JOHANSEN J.R. & FUČÍKOVÁ K., 2011 — *Tapinothrix clintonii* sp. nov. (Pseudanabaenaceae, Cyanobacteria), a new species at the nexus of five genera. *Fottea* 11: 127-140.

BRAY J.P., BROADY P.A., NIYOGI D.K. & HARDING J.S., 2008 — Periphyton communities in New Zealand streams impacted by acid mine drainage. *Marine and freshwater research* 59: 1084-1091.

CESCHI-BERRINI C., DE APPOLONIA F., DALLA VALLE L., KOMÁREK J. & ANDREOLI C., 2004 — Morphological and molecular characterization of a thermophilic cyanobacterium (Oscillatoriales) from Euganean Thermal Springs (Padua, Italy). *Algological studies* 113: 73-85.

CHONG C.W., CONVEY P., PEARCE D.A. & TAN I.K.P., 2012 — Assessment of soil bacterial communities on Alexander Island (in the maritime and continental Antarctic transitional zone). *Polar biology* 35: 387-399.

CHRISMAS N.A.M., ANESIO A.M. & SÁNCHEZ-BARACALDO P., 2012 — Multiple adaptations to polar and alpine environments within cyanobacteria: a phylogenomic and Bayesian approach. *Frontiers in microbiology* 6: 1070.

CIVITA M., CUCCHI F., EUSABIO A., GARAVOGLIA S., MARANZANA F. & VIGNA B., 1995 — The Timavo hydrogeologic system: an important reservoir of supplementary water resources to be reclaimed and protected. *Acta carsologica* 24: 169-186.

COLEMAN A.W., 2009 — Is there a molecular key to the level of ‘‘biological species” in eukaryotes? A DNA guide. *Molecular phylogenetics and evolution* 50: 197-203.

CUCCHI F., BIOLCHI S., ZINI L., JURKOVŠEK B.& KOLAR-JURKOVŠEK T., 2015 — Geologia e geomorfologia del Carso Classico/Geologija in geomorfologija klasičnega Krasa. In: Cucchi F., Zini L. & Calligaris C. (Eds), *Le acque del Carso Classico. Progetto Hydrokarst/ Vodonosnik Klasičnega Krasa. Projekt Hydrokarst*. Trieste, EUT Edizioni, Università di Trieste, pp. 23-52.

DARTY K., DENISE A. & PONTY Y., 2009 — VARNA: Interactive drawing and editing of the RNA secondary structure. *Bioinformatics* 25: 1974-1975.

DE LA TORRE J.R., GOEBEL B.M., FRIEDMANN E.I. & PACE N.R., 2003 — Microbial Diversity of Cryptoendolithic Communities from the McMurdo Dry Valleys, Antarctica. *Applied and environmental microbiology* 69: 3858-3867.

DOBÀT K., 1963 — "Höhlenalgen" bedrohen die Eiszeitmalereien von Lascaux. *Die Höhle* 14: 41-45.
DVOŘÁK P., JAHODÁŘOVÁ E., HAŠLER P., GUSEV E. & POULÍČKOVÁ A., 2015 — A new tropical cyanobacterium *Pinocchia polymorpha* gen. et sp. nov. derived from the genus *Pseudanabaena*. *Fottea, Olomouc* 15: 113-120.
FELSENSTEIN J., 1985 — Confidence limits on phylogenies: an approach using bootstrap. *Evolution* 39: 783-791.
EDGAR R.C., 2004 — MUSCLE: multiple sequence alignment with high accuracy and high throughput. *Nucleic acids research* 32: 1792-1797.
GUINDON S. & GASCUEL O., 2003 — A simple, fast and accurate algorithm to estimate large phylogenies by maximum likelihood. *Systematic biology* 52: 696-704.
HAUER T., MÜHLSTEINOVÁ R., BOHUNICKÁ M., KAŠTOVSKÝ J. & MAREŠ J., 2015 — Diversity of cyanobacteria on rock surfaces. *Biodiversity and conservation* 24: 759-779.
HERNÁNDEZ-MARINÉ M. & CANALS T., 1994 — *Herpyzonema pulverulentum* (Mastigocladaceae) a new cavernicolous atmophytic and limeincrusted cyanophyte. *Algological studies* 75: 123-136.
ITEMAN I., RIPPKA R., TANDEAU DE MARSAC N. & HERDMAN M., 2000 — Comparison of conserved structural and regulatory domains within divergent 16S-23S rRNA spacer sequences of cyanobacteria. *Microbiology* 146: 1275-1286.
JOHANSEN J.R., LOWE R.L., CARTY S., FUCIKOVA K., OLSEN C.E., FITZPATRICK M.H., RESS J.A. & FUREY P.C., 2007 — New algal species records for Great Smoky Mountains National Park, with an annotated checklist of all reported algal taxa for the park. *Southeastern naturalist* 6: 99-134.
JOHANSEN J.R., KOVACIK L., CASAMATTA D.A., FUČIKOVÁ K. & KAŠTOVSKÝ J., 2011 — Utility of 16S-23S ITS sequence and secondary structure for recognition of intrageneric and intergeneric limits within cyanobacterial taxa: *Leptolyngbya corticola* sp. nov. (Pseudanabaenaceae, Cyanobacteria). *Nova Hedwigia* 92: 283-302.
KLEINTEICH J., WOODB S.A., PUDDICK J., SCHLEHECK D., KÜPPER F.C. & DIETRICH D., 2013 — Potent toxins in Arctic environments – Presence of saxitoxins and an unusual microcystin variant in Arctic freshwater ecosystems. *Chemico-biological interactions* 206: 423-431.
KOMÁREK J. & ANAGNOSTIDIS K., 2005 — Cyanoprokaryota 2. Teil/2nd Part: Oscillatoriales. In: Büdel B., Krienitz L., Gärtner G. & Schagerl M. (Eds), *Süsswasserflora von Mitteleuropa 19/2*. Heidelberg, Elsevier/Spektrum, pp. 174-243.
KOMÁREK J., KAŠTOVSKÝ J., VENTURA S., TURICCHIA S. & ŠMARDA J., 2009 — The cyanobacterial genus *Phormidesmis*. *Algological studies* 129: 41-59.
KOMÁREK J., KAŠTOVSKÝ J., MAREŠ J. & JOHANSEN J. R., 2014 — Taxonomic classification of cyanoprokaryotes (cyanobacterial genera) 2014, using a polyphasic approach. *Preslia* 86: 295-335.
LAMPRINOU V., HERNÁNDEZ-MARINÉ M., CANALS T., KORMAS K., ECONOMOU-AMILLI A. & PANTAZIDOU A., 2011 — Morphology and molecular evaluation of *Iphinoe spelaeobios* gen. nov., sp. nov. and *Loriellopsis cavernicola* gen. nov., sp. nov., two stigonematalean cyanobacteria from Greek and Spanish caves. *International Journal of Systematic and evolutionary microbiology* 61: 2907-2915.
LAMPRINOU V., SKARAKI K., KOTOULAS G., ECONOMOU-AMILLI A. & PANTAZIDOU A., 2012a — *Toxopsis calypsus* gen. nov., sp. nov. (Cyanobacteria, Nostocales) from cave 'Francthi', Peloponnese, Greece: a morphological and molecular evaluation. *International Journal of speleology* 63: 2870-2877.
LAMPRINOU V., SKARAKI K., KOTOULAS G., ANAGNOSTIDIS K., ECONOMOU-AMILLI A. & PANTAZIDOU A., 2012b — A new species of *Phormidium* (Cyanobacteria, Oscillatoriales) from three Greek Caves: morphological and molecular analysis. *Fundamental and applied limnology* 182/2: 109-116.
LAMPRINOU V., SKARAKI K., KOTOULAS G., ANAGNOSTIDIS K., ECONOMOU-AMILLI A. & PANTAZIDOU A., 2013 — A new species of *Phormidium* (Cyanobacteria, Oscillatoriales) from Greek Caves – morphological and molecular evaluation. *Fundamental and applied limnology* 182: 109-116.
LAMPRINOU V., DANIELIDIS D.B., PANTAZIDOU A., OIKONOMOU A. & ECONOMOU-AMILLI A., 2014 — The show cave of Diros vs. wild caves of Peloponnese, Greece – distribution patterns of Cyanobacteria. *International journal of speleology* 43: 335-342.
LEE N.M., MEISINGER D.B., AUBRECHT R., KOVÁČIK L., SAIZ-JIMENEZ C., BASKAR S., BASKAR R., LIEBL W., PORTER M. & ENGEL A.S., 2012 — Caves and Karst environments. In: Bell E.M. (Ed.), *Life at Extremes: Environments, Organisms and Strategies for Survival*. Wallingford, CAB International, pp. 320-344.

LOWE T.M. & EDDY S.R., 1997 — tRNAscan-SE: A Program for Improved Detection of Transfer RNA Genes in Genomic Sequence. *Nucleic acids research* 25: 955-964.

MADDISON W.P. & MADDISON D.R., 2009 — Mesquite: A modular system for evolutionary analysis, version 2.71. Available at: http://mesquiteproject.org (01 March 2010).

MARTINEAU E., WOOD S.A., MILLER M.R., JUNGBLUT A.D., HAWES I., WEBSTER-BROWN J., PACKER M.A., 2013 — Characterisation of Antarctic cyanobacteria and comparison with New Zealand strains. *Hydrobiologia* 711: 139-154.

MERICAN F., 2013 — *A Taxonomic and Ecological Study of Periphytic Cyanobacteria in Kaituna River and Its Tributaries, Banks Peninsula, New Zealand*. Ph. D. Thesis, University of Canterbury.

MISCOE L.H., JOHANSEN J.R., VACCARINO M.A., PIETRASIAK N. & SHERWOOD A.R., 2016 — Novel cyanobacteria from caves on Kauai, Hawaii. *Bibliotheca phycologica* 120: 75-152.

MORO I., RASCIO N., LA ROCCA N., DI BELLA M. & ANDREOLI C., 2007 — *Cyanobacterium aponinum*, a new Cyanoprokaryote from the microbial mat of Euganean thermal springs (Padua, Italy). *Algological studies* 123: 1-15.

MORO I., RASCIO N., LA ROCCA N., SCIUTO K., ALBERTANO P., BRUNO L. & ANDREOLI C., 2010 — Polyphasic characterization of a thermo-tolerant filamentous cyanobacterium isolated from the Euganean thermal muds (Padova, Italy). *European journal of phycology* 45: 143-154.

MULEC J., KOSI G. & VRHOVŠEK D., 2008 — Characterization of cave aerophytic algal communities and effects of irradiance levels on production of pigments. *Journal of cave and karst studies* 70: 3-12.

MÜLLER T., PHILIPPI N., DANDEKAR T., SCHULTZ J. & WOLF M., 2007 — Distinguishing species. *RNA* 13: 1469-1472.

OLSSON-FRANCIS K., DE LA TORRE R. & COCKELL C.S., 2010 — Isolation of Novel Extreme-Tolerant Cyanobacteria from a Rock-Dwelling Microbial Community by Using Exposure to Low Earth Orbit. *Applied and environmental microbiology* 76: 2115-2121.

OSORIO-SANTOS K., PIETRASIAK N., BOHUNICKÁ M., MISCOE L.H., KOVÁČIK L., MARTIN M.P. & JOHANSEN J.R., 2014 — Seven new species of *Oculatella* (Pseudanabaenales, Cyanobacteria): taxonomically recognizing cryptic diversification. *European journal of phycology* 49: 450-470.

PERKERSON R., JOHANSEN J.R., KOVÁČIK L., BRAND J., KAŠTOVSKÝ J. & CASAMATTA D., 2011 — A unique Pseudanabaenalean (Cyanobacteria) genus *Nodosilinea* gen. nov. based on morphological and molecular data. *Journal of phycology* 47: 1397-1412.

POSADA D., 2008 — jModelTest: phylogenetic model averaging. *Molecular biology and evolution* 25: 1253-1256.

POSADA D. & BUCKLEY T.R., 2004 — Model selection and model averaging in phylogenetics: advantages of the AIC and Bayesian approaches over likelihood ratio tests. *Systematic biology* 53: 793-808.

POSADA D. & CRANDALL K.A., 1998 — Modeltest: Testing the model of DNA substitution. *Bioinformatics* 14: 817-818.

RAMBAUT A. & DRUMMOND A.J., 2007 — Tracer, version 1.5. Available at: http://beast.bio.ed.ac.uk/Tracer (01 December 2009).

REUTER J.S. & MATHEWS D.H., 2010 — RNAstructure: software for RNA secondary structure prediction and analysis. *BMC Bioinformatics* 11: 129.

RIPPKA R., DERUELLES J., WATERBURY J.B., HERDMAN M. & STANIER R.Y., 1979 — Generic assignments, strain histories and properties of pure cultures of Cyanobacteria. *Journal of general microbiology* 111: 1-61.

RONQUIST F. & HUELSENBECK J.P., 2003 — MrBayes 3: bayesian phylogenetic inference under mixed models. *Bioinformatics* 19: 1572-1574.

SAIZ-JIMENEZ C., 2012 — Microbiological and environmental issues in show caves. *World Journal of microbiology and biotechnology* 28: 2453-2464.

SANT'ANNA C.L., BRANCO L.H.Z. & SILVA S.M.F., 1991 — A new species of *Gloeothece* (Cyanophyceae, Microcystaceae) from São Paulo State, Brazil. *Algological studies* 62: 1-5.

SAW J.H.W., SCHATZ M., BROWN M.V., KUNKEL D.D., FOSTER J.S., SHICK H., CHRISTENSEN S., HOU S., WAN X. & DONACHIE S.P., 2013 — Cultivation and Complete Genome Sequencing of *Gloeobacter kilaueensis* sp. nov., from a Lava Cave in Kīlauea Caldera, Hawai'i. *PLoS ONE* 8: e76376.

SCHATTNER P., BROOKS A.N. & LOWE T.M., 2005 — The tRNAscan-SE, snoscan and snoGPS web servers for the detection of tRNAs and snoRNAs. *Nucleic acids research* 33: W686-689.

SCHMIDT S.K., LYNCH R.C., KING A.J., KARKI D., ROBESON M.S., NAGY L., WILLIAMS M.W., MITTER M.S. & FREEMAN K.R., 2011 — Phylogeography of microbial phototrophs in the dry valleys of the high Himalayas and Antarctica. *Proceedings of the royal society B* 278: 702-708.

SCHWARZ G., 1978 — Estimating the dimension of a model. *The Annals of Statistics* 6: 461-464.

SCIUTO K. & MORO I., 2016 — Detection of the new cosmopolitan genus *Thermoleptolyngbya* (Cyanobacteria, Leptolyngbyaceae) using the 16S rRNA gene and 16S-23S ITS region. *Molecular phylogenetics and evolution* 105: 15-35.

SHERWOOD A.R., CONKLIN K.Y. & LIDDY Z.J., 2014 — What's in the air? Preliminary analyses of Hawaiian airborne algae and land plant spores reveal a diverse and abundant flora. *Phycologia* 53: 579-582.

SMITH M.C., BOWMAN J.P., SCOTT F.J. & LINE M.A., 2000 — Sublithic bacteria associated with Antarctic quartz stones. *Antarctic science* 12: 177-184.

SMRŽ J., KOVÁČ Ľ., MIKEŠ J. & LUKEŠOVÁ A., 2013 — Microwhip Scorpions (Palpigradi) Feed on Heterotrophic Cyanobacteria in Slovak Caves – A Curiosity among Arachnida. *PLoS ONE* 8: e75989.

STACKEBRANDT E. & GOEBEL B.M., 1994 — Taxonomic note: a place for DNA-DNA reassociation and 16S rRNA sequence analysis in the present species definition in bacteriology. *International journal of systematic bacteriology* 44: 846-849.

TAMURA K., PETERSON D., PETERSON N., STECHER G., NEI M. & KUMAR S., 2011 — MEGA5: molecular Evolutionary Genetics Analysis using maximum likelihood, evolutionary distance, and maximum parsimony methods. *Molecular biology and evolution* 28: 2731-2739.

TATON A., GRUBISIC S., BRAMBILLA E., DE WIT R. & WILMOTTE A., 2003 — Cyanobacterial Diversity in Natural and Artificial Microbial Mats of Lake Fryxell (McMurdo Dry Valleys, Antarctica): a Morphological and Molecular Approach. *Applied and environmental microbiology* 69: 5157-5169.

TATON A., GRUBISIC S., BALTHASART P., HODGSON D.A., LAYBOURN-PARRY J. & WILMOTTE A., 2006a — Biogeographical distribution and ecological ranges of benthic cyanobacteria in East Antarctic lakes. *FEMS microbiology ecology* 57: 272-289.

TATON A., GRUBISIC S., ERTZ D., HODGSON D. A., PICCARDI R., BIONDI N., TREDICI M. R., MAININI M., LOSI D., MARINELLI F. & WILMOTTE A., 2006b — Polyphasic study of Antarctic cyanobacterial strains. *Journal of phycology* 42: 1257-1270.

TATON A., WILMOTTE A., ŠMARDA J., ELSTER J. & KOMÁREK J., 2011 — *Plectolyngbya hodgsonii*: a novel filamentous cyanobacterium from Antarctic lakes. *Polar biology* 34: 181-191.

TURICCHIA S., VENTURA S., KOMÁRKOVÁ J. & KOMÁREK J., 2009 — Taxonomic evaluation of cyanobacterial microflora from alkaline marshes of northern Belize. 2. Diversity of oscillatorialean genera. *Nowa Hedwigia* 89: 165-200.

TURNER S., 1997 — Molecular systematics of oxygenic photosynthetic bacteria. *Plant systematics and evolution* 11 (Supplement): 13-52.

VAZ M.G.G.V., GENUÁRIO D.B., ANDREOTE A.P.D.A., MALONE C.F.S., SANT'ANNA A.L., BARBIERO L. & FIORE M.F., 2015 — *Pantanalinema* gen. nov. and *Alkalinema* gen. nov.: novel pseudanabaenacean genera (Cyanobacteria) isolated from saline-alkaline lakes. *International Journal of systematic and evolutionary microbiology* 65: 298-308.

WILMOTTE A., 1991 — Taxonomic study of marine oscillatoriacean strains (Cyanophyceae, Cyanobacteria) with narrow trichomes. I. Morphological variability and autecological features. *Algological studies* 64: 215–248.

WOLF M., CHEN S., SONG J., ANKENBRAND M. & MÜLLER T., 2013 — Compensatory Base Changes in ITS2 Secondary Structures Correlate with the Biological Species Concept Despite Intragenomic Variability in ITS2 Sequences – A Proof of Concept. *PLoS ONE* 8: e66726.

ZAMMIT G., BILLI D. & ALBERTANO P., 2012 — The subaerophytic cyanobacterium *Oculatella subterranea* (Oscillatoriales, Cyanophyceae) gen. et sp. nov.: a cytomorphological and molecular description. *European journal of phycology* 47: 341-354.